

Testing new physics with the electron $g - 2$

G.F. Giudice,^a P. Paradisi^a and M. Passera^b

^a*CERN, Theory Division,
1211 Geneva 23, Switzerland*

^b*Istituto Nazionale Fisica Nucleare,
35131 Padova, Italy*

E-mail: Gian.Giudice@cern.ch, paride.paradisi@cern.ch,
passera@pd.infn.it

ABSTRACT: We argue that the anomalous magnetic moment of the electron (a_e) can be used to probe new physics. We show that the present bound on new-physics contributions to a_e is 8×10^{-13} , but the sensitivity can be improved by about an order of magnitude with new measurements of a_e and more refined determinations of α in atomic-physics experiments. Tests on new-physics effects in a_e can play a crucial role in the interpretation of the observed discrepancy in the anomalous magnetic moment of the muon (a_μ). In a large class of models, new contributions to magnetic moments scale with the square of lepton masses and thus the anomaly in a_μ suggests a new-physics effect in a_e of $(0.7 \pm 0.2) \times 10^{-13}$. We also present examples of new-physics theories in which this scaling is violated and larger effects in a_e are expected. In such models the value of a_e is correlated with specific predictions for processes with violation of lepton number or lepton universality, and with the electric dipole moment of the electron.

KEYWORDS: Supersymmetry Phenomenology

Contents

1	Introduction	1
2	Status of the electron $g - 2$	2
2.1	The experimental situation	2
2.2	The standard model prediction	3
2.2.1	QED contribution	3
2.2.2	Electroweak and hadronic contributions	4
2.2.3	Standard Model prediction of a_e and value of α	5
2.2.4	Standard Model vs. measurement	6
3	New Physics tests with a_e	6
3.1	Future improvements in the determination of Δa_e	7
3.2	General structure of new-physics contributions	7
3.3	Status of the τ anomalous magnetic moment	10
4	Supersymmetry and a_e	11
4.1	Lepton flavor conserving case	11
4.1.1	Correlation between a_e and violation of lepton universality in LFC	13
4.2	Lepton flavor violating case	15
4.2.1	Correlation between a_e and $\tau \rightarrow e\gamma$ in LFV	16
4.2.2	Correlation between a_e and violation of lepton universality in LFV	19
4.3	Disoriented A-terms	19
5	Light (pseudo)scalars and a_e	21
5.1	One-loop effects	22
5.2	Two-loop effects	23
6	Vector-like fermions and a_e	25
7	Conclusions	27
A	Loop functions	28

1 Introduction

The anomalous magnetic moment of the muon $a_\mu = (g-2)_\mu/2$ is one of the most celebrated tests of the Standard Model (SM). Indeed, the high precision of its theoretical and experimental determinations makes a_μ a powerful test on new physics. The situation has become

especially intriguing with the $\sim 3.5\sigma$ reported discrepancy between the SM prediction and the experimental value [1–7]

$$\Delta a_\mu = a_\mu^{\text{EXP}} - a_\mu^{\text{SM}} = 2.90(90) \times 10^{-9}. \quad (1.1)$$

On the other hand, the anomalous magnetic moment of the electron a_e has never played a role in testing ideas beyond the SM. In fact, it is believed that new-physics contaminations of a_e are too small to be relevant and, with this assumption, the measurement of a_e is employed to determine the value of the fine-structure constant α .

The aim of this paper is to emphasize that the situation has now changed, thanks to advancements both on the theoretical and experimental sides. Indeed, the theoretical prediction of a_e has been refined to an unprecedented accuracy and its experimental value is now known with smaller errors. At the same time, good determinations of the fine-structure constant have been obtained from atomic physics experiments, providing a value of α that is completely independent of the measurements of a_e . As a result, a_e can now be viewed as a very useful probe of physics beyond the SM and the situation is going to become even more promising soon, as efforts are underway to reduce significantly both theoretical and experimental errors. The most exciting aspect of the story is that a_e will soon provide us with a crucial consistency check of new-physics interpretations of the alleged discrepancy in a_μ . Moreover, in certain classes of models, if Δa_μ is caused by new physics, then it is possible to correlate the value of a_e with various other rare processes violating lepton universality or individual lepton number.

The paper is organized as follows. In section 2 we carefully review the present status of the SM prediction of a_e and confront it with the experimental measurement. In section 3 we discuss future improvements in the theoretical and experimental results and show their impact for probing new physics. We use the prototype examples of supersymmetry (section 4), of a light pseudoscalar (section 5), and of vector-like fermions (section 6) to illustrate generic features of theories beyond the SM. Our results are summarized in section 7.

2 Status of the electron $g - 2$

2.1 The experimental situation

The classic series of measurements of the electron and positron anomalous magnetic moments carried out at the University of Washington yielded in 1987 the value $a_e^{\text{EXP}} = 115\,965\,218\,83(42) \times 10^{-13}$ [8, 9]. More recently, a new determination of the electron $g-2$ has been performed by Gabrielse and his collaborators at Harvard University, with the result [10–12]

$$a_e^{\text{EXP}} = 115\,965\,218\,07.3(2.8) \times 10^{-13}. \quad (2.1)$$

The uncertainty of this result, $\delta a_e^{\text{EXP}} = 2.8 \times 10^{-13}$, i.e. 0.24 parts in a billion (ppb), is 15 times smaller than that reported back in 1987. The two measurements differ by 1.8 standard deviations.

2.2 The standard model prediction

The SM prediction a_e^{SM} is usually split into three parts: QED, electroweak (EW) and hadronic. Here we provide a summary of the present status of these contributions.

2.2.1 QED contribution

The QED term a_e^{QED} arises from the subset of SM diagrams containing only leptons and photons. This dimensionless quantity can be cast in the general form [13]

$$a_e^{\text{QED}} = A_1 + A_2 \left(\frac{m_e}{m_\mu} \right) + A_2 \left(\frac{m_e}{m_\tau} \right) + A_3 \left(\frac{m_e}{m_\mu}, \frac{m_e}{m_\tau} \right), \quad (2.2)$$

where m_e , m_μ and m_τ are the electron, muon and tau lepton masses. The term A_1 , arising from diagrams containing only photons and electrons, is mass and flavor independent. In contrast, the terms A_2 and A_3 , generated by graphs containing also muons and taus, are functions of the indicated mass ratios. The muon contribution to a_e^{QED} , although suppressed by $m_e^2/m_\mu^2 \sim 2.34 \times 10^{-5}$, is about ten times larger than the experimental uncertainty in eq. (2.1) (the tau contribution, suppressed by m_e^2/m_τ^2 , is of order 10^{-14}). The functions A_i ($i = 1, 2, 3$) can be expanded as power series in α/π and computed order-by-order: $A_i = A_i^{(2)} (\alpha/\pi) + A_i^{(4)} (\alpha/\pi)^2 + A_i^{(6)} (\alpha/\pi)^3 + \dots$.

Only one diagram is involved in the evaluation of the one-loop (first-order in α , second-order in the electric charge) contribution; it provides the famous result by Schwinger [14]

$$C_1 = A_1^{(2)} = 1/2. \quad (2.3)$$

Seven two-loop diagrams contribute to the fourth-order coefficient $A_1^{(4)}$, one to $A_2^{(4)}(m_e/m_\mu)$ and one to $A_2^{(4)}(m_e/m_\tau)$, while $A_3^{(4)}(m_e/m_\mu, m_e/m_\tau) = 0$. The exact mass-independent coefficient has been known for more than fifty years, $A_1^{(4)} = 197/144 + \pi^2/12 + 3\zeta(3)/4 - (\pi^2/2) \ln 2 = -0.328\,478\,965\,579\,193\,78\dots$ [15–18], where $\zeta(s)$ is the Riemann zeta function. The numerical evaluation of the exact expression for the mass-dependent coefficient $A_2^{(4)}$ [19, 20] with the latest CODATA recommended mass ratios $m_e/m_\mu = 4.836\,331\,66(12) \times 10^{-3}$ and $m_e/m_\tau = 2.875\,92(26) \times 10^{-4}$ yields $A_2^{(4)}(m_e/m_\mu) = 5.197\,386\,68(26) \times 10^{-7}$ and $A_2^{(4)}(m_e/m_\tau) = 1.837\,98(33) \times 10^{-9}$ [21]. The tiny errors are due to the uncertainties of the mass ratios. The sum of the above values provides the two-loop QED coefficient

$$C_2 = A_1^{(4)} + A_2^{(4)}(m_e/m_\mu) + A_2^{(4)}(m_e/m_\tau) = -0.328\,478\,444\,002\,55(33). \quad (2.4)$$

The standard error $\delta C_2 = 3.3 \times 10^{-13}$ leads to a totally negligible $O(10^{-18})$ uncertainty in a_e^{QED} .

More than one hundred diagrams are involved in the evaluation of the three-loop (sixth-order) QED contribution. The exact result for the coefficient $A_1^{(6)}$, mainly due to Remiddi and his collaborators [22], yields the numerical value $A_1^{(6)} = 1.181\,241\,456\,587\dots$. The analytic calculation of the mass-dependent coefficient $A_2^{(6)}(r)$ for arbitrary values of the mass ratio r was completed in 1993 by Laporta and Remiddi [23, 24]. The exact formula contains hundreds of polylogarithmic functions, including harmonic polylogarithms [25–28].

Numerically evaluating these analytic expressions with the latest CODATA mass ratios given above, we obtain $A_2^{(6)}(m_e/m_\mu) = -7.373\,941\,62(27) \times 10^{-6}$ and $A_2^{(6)}(m_e/m_\tau) = -6.5830(11) \times 10^{-8}$. The same values can be obtained with the simple series expansions of [29], thus avoiding the complexities of these numerical evaluations. The contribution to a_e^{QED} of these three-loop mass-dependent coefficients is -0.9×10^{-13} , i.e. about a third of the present experimental uncertainty δa_e^{EXP} , see eq. (2.1). The contribution of the three-loop diagrams with both muon and tau loop insertions in the photon propagator can be calculated numerically from the integral expressions of [30]. We get $A_3^{(6)}(m_e/m_\mu, m_e/m_\tau) = 1.909\,82(34) \times 10^{-13}$, a totally negligible $O(10^{-21})$ contribution to a_e^{QED} . Adding up all the above values we obtain the three-loop QED coefficient

$$C_3 = 1.181\,234\,016\,816(11). \tag{2.5}$$

The error $\delta C_3 = 1.1 \times 10^{-11}$ leads to a totally negligible $O(10^{-19})$ uncertainty in a_e^{QED} .

Almost one thousand four-loop diagrams contribute to the mass-independent coefficient $A_1^{(8)}$, and only few of them are known analytically. However, in a formidable effort that has its origins in the 1960s, Kinoshita and his collaborators calculated $A_1^{(8)}$ numerically [31, 32]. Their latest result is $A_1^{(8)} = -1.9106(20)$, from ref. [33]. In the same, very recent, article they also computed the tiny mass-dependent four-loop coefficients $A_2^{(8)}(m_e/m_\mu) = 9.222(66) \times 10^{-4}$, $A_2^{(8)}(m_e/m_\tau) = 8.24(12) \times 10^{-6}$, and $A_3^{(8)}(m_e/m_\mu, m_e/m_\tau) = 7.465(18) \times 10^{-7}$. Adding up these values one gets

$$C_4 = -1.9097(20). \tag{2.6}$$

The error $\delta C_4 = 0.0020$, caused by the numerical procedure, leads to an uncertainty of 5.8×10^{-14} in a_e^{QED} . Independent work on the computation of the four-loop coefficient is in progress [34].

Very recently, Kinoshita and his collaborators completed the heroic calculation of the 12672 five-loop diagrams contributing to the tenth-order coefficient $A_1^{(10)}$ [33, 35–46]. Their result is $A_1^{(10)} = 9.16(58)$. They also computed the tiny mass-dependent term $A_2^{(10)}(m_e/m_\mu) = -0.003\,82(39)$. As the tenth-order contribution of the τ lepton loops can be safely neglected, the sum of these two numbers provides the five-loop coefficient

$$C_5 = 9.16(58). \tag{2.7}$$

The error $\delta C_5 = 0.58$ leads to an uncertainty of 3.9×10^{-14} in a_e^{QED} .

The complete QED contribution is given by

$$a_e^{\text{QED}}(\alpha) = \sum_{i=1}^{\infty} C_i (\alpha/\pi)^i. \tag{2.8}$$

As $(\alpha/\pi)^6 = 1.6 \times 10^{-16}$, terms of order $i \geq 6$ are assumed to be negligible at present.

2.2.2 Electroweak and hadronic contributions

The electroweak contribution is [21, 47, 48]

$$a_e^{\text{EW}} = 0.2973(52) \times 10^{-13}. \tag{2.9}$$

This precise value includes the two-loop contributions first computed in [47, 48].

The hadronic term,

$$a_e^{\text{HAD}} = 16.82(16) \times 10^{-13}, \tag{2.10}$$

is six times larger than the present experimental uncertainty δa_e^{EXP} , see eq. (2.1). It is the sum of the following three contributions: the leading-order one, $18.66(11) \times 10^{-13}$, very recently updated in [49] (see also [5]), the higher-order vacuum-polarization part, $-2.234(14) \times 10^{-13}$ [49] (see also [5, 50]), and the hadronic light-by-light term, $0.39(13) \times 10^{-13}$ [5] (see also [51]).

2.2.3 Standard Model prediction of a_e and value of α

The sum of the QED contribution $a_e^{\text{QED}}(\alpha)$ plus the hadronic and weak terms discussed above yields the SM prediction of the electron $g-2$:

$$a_e^{\text{SM}}(\alpha) = a_e^{\text{QED}}(\alpha) + a_e^{\text{EW}} + a_e^{\text{HAD}} \tag{2.11}$$

(the dependence on α of any contribution other than a_e^{QED} is negligible). To compare it with experiment, we need the value of the fine-structure constant α . The latest determination of α by CODATA [21],

$$\alpha(\text{CODATA}) = 1/137.035\,999\,074(44) [0.32 \text{ ppb}], \tag{2.12}$$

cannot be employed for our purpose, as it is mainly driven by the value obtained equating the theoretical SM prediction of the electron $g-2$ with its measured value,

$$a_e^{\text{SM}}(\alpha) = a_e^{\text{EXP}} \tag{2.13}$$

(thus assuming the absence of any significant new-physics contribution).¹ Indeed, solving eq. (2.13) with the experimental value of eq. (2.1) we obtain

$$\alpha(g-2) = 1/137.035\,999\,173(34) [0.25 \text{ ppb}], \tag{2.14}$$

in agreement with ref. [33]. This is the most precise value of α available today. The difference between this number and $\alpha(\text{CODATA})$ in eq. (2.12) is mainly due to the very recent QED five-loop result of ref. [33], which is included in our derivation, but not in the CODATA one.

Clearly, in order to compute $a_e^{\text{SM}}(\alpha)$ and compare it with a_e^{EXP} we must use a determination of α independent of the electron $g-2$. At present, the two most accurate ones are

$$\alpha(^{133}\text{Cs}) = 1/137.036\,000\,0(11) [7.7 \text{ ppb}], \tag{2.15}$$

$$\alpha(^{87}\text{Rb}) = 1/137.035\,999\,049(90) [0.66 \text{ ppb}]. \tag{2.16}$$

They differ by less than one standard deviation. The first value was obtained from the ratio h/M_{Cs} (h is Planck's constant and M_{Cs} is the mass of the ^{133}Cs atom), which was

¹The identical value presently reported by the Particle Data Group (PDG) [52], adopted from CODATA, cannot be used either.

determined by measuring the atomic recoil frequency shift of photons absorbed or emitted by ^{133}Cs atoms using atom interferometry [53]. The second was deduced from the measurement of the ratio h/M_{Rb} (M_{Rb} is the mass of the ^{87}Rb atom) with an experimental scheme that combines atom interferometry with Bloch oscillation [54–56]. The values of α in eqs. (2.15), (2.16) were inferred from the ratios $h/M_{\text{Cs,Rb}}$ combining them with the very precisely known Rydberg constant and the mass ratios $M_{\text{Cs,Rb}}/m_e$ [21]. Given the higher precision of $\alpha(^{87}\text{Rb})$ vs. $\alpha(^{133}\text{Cs})$ (by more than one order of magnitude), the former is the value of α we employ to compute $a_e^{\text{SM}}(\alpha)$. We note that $\alpha(^{87}\text{Rb})$ agrees with $\alpha(g-2)$ in eq. (2.14) (the difference is 1.3 standard deviations), and its uncertainty $\delta\alpha(^{87}\text{Rb})$ is larger than $\delta\alpha(g-2)$ just by a factor of 2.7.

The SM prediction $a_e^{\text{SM}}(\alpha)$, computed with the fine-structure constant value $\alpha(^{87}\text{Rb})$ of eq. (2.16), is

$$a_e^{\text{SM}} = 115\,965\,218\,17.8 (0.6)(0.4)(0.2)(7.6) \times 10^{-13}. \quad (2.17)$$

The first (second) error is determined by the uncertainty of the four(five)-loop QED coefficient, the third one is δa_e^{HAD} , and the last (7.60×10^{-13}) is caused by the error $\delta\alpha(^{87}\text{Rb})$. The uncertainties of the EW and two/three-loop QED contributions are totally negligible. When combined in quadrature, all these uncertainties yield $\delta a_e^{\text{SM}} = 7.64 \times 10^{-13}$. Note that the present precision of the SM prediction, which is about three times worse than the experimental one, is limited by the uncertainty of the fine-structure constant $\alpha(^{87}\text{Rb})$.

2.2.4 Standard Model vs. measurement

The SM value in eq. (2.17) is in good agreement with the experimental one in eq. (2.1). They differ by

$$\Delta a_e = a_e^{\text{EXP}} - a_e^{\text{SM}} = -10.5 (8.1) \times 10^{-13}, \quad (2.18)$$

i.e. 1.3 standard deviations, thus providing a beautiful test of QED at four-loop level! (The four-loop contribution to a_e^{QED} is -5.56×10^{-11} .) Once again, the uncertainty $\delta\Delta a_e = 8.1 \times 10^{-13}$ is dominated by that of the SM prediction, through the error caused by $\delta\alpha(^{87}\text{Rb})$.

3 New Physics tests with a_e

New physics effects in the electron $g-2$ are usually expected to be comparable with the EW contribution, $a_e^{\text{EW}} = 0.2973 (52) \times 10^{-13}$, see eq. (2.9), and therefore much smaller than the uncertainty $\delta\Delta a_e = 8.1 \times 10^{-13}$ reported above. Indeed, as we mentioned earlier, the commonly used CODATA (and PDG) value of α is mainly derived from a_e^{EXP} under this assumption. However, as we will discuss in the next section, the uncertainty in Δa_e is expected to be reduced. Then, the anomalous magnetic moment of the electron will provide us with important information on new physics effects.

3.1 Future improvements in the determination of Δa_e

As we showed in sections 2.2.3 and 2.2.4, the uncertainty $\delta\Delta a_e = 8.1 \times 10^{-13}$ is the result of the combination, in quadrature, of the following errors, in units of 10^{-13} :

$$\underbrace{(0.6)_{\text{QED4}}, (0.4)_{\text{QED5}}, (0.2)_{\text{HAD}}, (7.6)_{\delta\alpha}, (2.8)_{\delta a_e^{\text{EXP}}}}_{(0.7)_{\text{TH}}} \tag{3.1}$$

The first one, 0.6×10^{-13} , is caused by the numerical procedure used to determine the four-loop QED coefficient. It is already rather small and can be further reduced to 0.1×10^{-13} with a large scale numerical recalculation [57]. Also the second error, induced by the five-loop QED term recently computed by Kinoshita and his collaborators, is already small, and may soon drop to less than 0.1×10^{-13} [57]. As the tiny — but hard to reduce — hadronic uncertainty is 0.16×10^{-13} and those of the EW and two/three-loop QED contributions are totally negligible, the overall purely theoretical error of Δa_e (i.e. the value of $\delta\Delta a_e$ obtained setting to zero δa_e^{EXP} and the error induced by $\delta\alpha$) is, at present, 0.7×10^{-13} . This is likely to decrease even further, by a factor of two or three, in a relatively near future.

Thanks to these recent theoretical improvements, the precision on Δa_e is now limited only by the experimental uncertainties δa_e^{EXP} and $\delta\alpha$. At present they affect $\delta\Delta a_e$ by 2.8×10^{-13} (δa_e^{EXP}) and 7.6×10^{-13} ($\delta\alpha$). It seems reasonable to expect a reduction of the former error to a part in 10^{-13} (or better) in ongoing efforts to improve the measurement of the electron (and positron) anomalous magnetic moment [58, 59]. Work is also in progress for a significant reduction of the latter error [56, 60].

In conclusion, a determination of Δa_e at the level of 10^{-13} (or below) is a goal that can be achieved not too far in the future with ongoing experimental work. As we will discuss in the next section, this will bring a_e to play a pivotal role in probing new physics in the leptonic sector.

3.2 General structure of new-physics contributions

The one-loop SM electroweak contribution to the anomalous magnetic moment of the lepton ℓ ($\ell = e, \mu, \tau$) is

$$(a_\ell^{\text{EW}})_{\text{1loop}} = \frac{m_\ell^2}{(4\pi v)^2} \left(1 - \frac{4}{3} \sin^2 \theta_W + \frac{8}{3} \sin^4 \theta_W \right) \approx 2 \times 10^{-9} \frac{m_\ell^2}{m_\mu^2}, \tag{3.2}$$

where $v = 174$ GeV. This can be viewed as a benchmark for contributions from new physics at the electroweak scale. For the muon, this is about the same size as the observed discrepancy, see eq. (1.1).

New physics effects for the leptonic $g-2$ can be accounted for by means of the effective Lagrangian

$$\mathcal{L} = e \frac{m_\ell}{2} (\bar{\ell}_R \sigma_{\mu\nu} A_{\ell\ell'} \ell'_L + \bar{\ell}'_L \sigma_{\mu\nu} A_{\ell\ell'}^* \ell_R) F^{\mu\nu} \quad \ell, \ell' = e, \mu, \tau, \tag{3.3}$$

which describes dipole transitions ($\ell \rightarrow \ell' \gamma$) in the leptonic sector. Starting from eq. (3.3), we can evaluate Δa_ℓ as

$$\Delta a_\ell = 2m_\ell^2 \text{Re}(A_{\ell\ell}). \tag{3.4}$$

Let us consider now some new particles with typical mass Λ_{NP} and couplings g_ℓ^L and g_ℓ^R to left- and right-handed leptons ℓ , respectively. The one-loop new-physics contribution to the amplitude $A_{\ell\ell'}$ is then of the form

$$A_{\ell\ell'} = \frac{1}{(4\pi \Lambda_{\text{NP}})^2} \left[(g_{\ell k}^L g_{\ell' k}^{L*} + g_{\ell k}^R g_{\ell' k}^{R*}) f_1(x_k) + \frac{v}{m_\ell} (g_{\ell k}^L g_{\ell' k}^{R*}) f_2(x_k) \right], \quad (3.5)$$

and therefore Δa_ℓ reads now

$$\Delta a_\ell = \frac{2m_\ell^2}{(4\pi \Lambda_{\text{NP}})^2} \left[(|g_{\ell k}^L|^2 + |g_{\ell k}^R|^2) f_1(x_k) + \frac{v}{m_\ell} \text{Re} (g_{\ell k}^L g_{\ell k}^{R*}) f_2(x_k) \right]. \quad (3.6)$$

With $f_{1,2}$ we indicate loop functions which depend on ratios (x_k) of unknown masses of the new particles contributing to the amplitude $\ell \rightarrow \ell' \gamma$, and k is a lepton flavor index. In the term proportional to f_1 , the chiral flip required by the dipole transition occurs through a mass insertion in the external lepton line. In the term proportional to f_2 , the mass insertion is in the internal line of some new particle, thus explaining the parametric factor v/m_ℓ . Although f_2 must be proportional to the lepton Yukawa coupling, as a consequence of chiral symmetry, in practice this term can become very sizeable whenever a new large coupling leads to a chiral enhancement.

In a broad class of theories beyond the SM, $g_\ell^{L,R}$ and f_1 are flavor universal (i.e. are the same for any ℓ) and f_2 vanishes, such that

$$\frac{\Delta a_{\ell_i}}{\Delta a_{\ell_j}} = \left(\frac{m_{\ell_i}}{m_{\ell_j}} \right)^2. \quad (3.7)$$

We will refer to this case as “naive scaling” (NS). NS applies, for instance, if the new particles have an underlying SU(3) flavor symmetry in their mass spectrum and in their couplings to leptons (which is the case for gauge interactions).

An interesting consequence of NS is that an explanation of the muon $g-2$ anomaly makes definite predictions for new effects in the anomalous magnetic moments of electron and τ ,

$$\Delta a_e = \left(\frac{\Delta a_\mu}{3 \times 10^{-9}} \right) 0.7 \times 10^{-13}, \quad (3.8)$$

$$\Delta a_\tau = \left(\frac{\Delta a_\mu}{3 \times 10^{-9}} \right) 0.8 \times 10^{-6}. \quad (3.9)$$

It is very exciting that the sensitivity in Δa_e is not far from what is required to test whether the discrepancy in the muon $g-2$ also manifests itself in the electron $g-2$ under the NS hypothesis. Thus, determining Δa_e with a precision below 10^{-13} is an important goal with rich physics consequences. The measurement of a_τ may play a similar role if a precision below 10^{-6} will be attained (see section 3.3).

Although the NS case is especially simple and common to a large class of new-physics interactions, it is by no means the only possibility. Many theories make predictions beyond NS, either because of the chirally-enhanced term proportional to f_2 , or because of lepton non-universality in the couplings ($g_\ell^{L,R}$) or the mass spectrum (f_1). For instance,

in a multi-Higgs doublet model, the couplings $g_\ell^{L,R}$ are related to Yukawa couplings and therefore one would find the scaling $\Delta a_{\ell_i}/\Delta a_{\ell_j} = m_{\ell_i}^4/m_{\ell_j}^4$. A different example is offered by supersymmetry with non-degenerate sleptons, in which Δa_ℓ loses its correlation with lepton masses.

The case of non-naive scaling is interesting from the theoretical point of view because it allows for exploration of the structure of lepton symmetries. It is also interesting experimentally because it can lead to effects in Δa_e testable already with present sensitivity. Moreover, as we will show with various examples in the next sections, any lepton non-universality in Δa_ℓ can be related to other experimental observables, offering the possibility of cross-checking new physics effects.

The underlying $\ell \rightarrow \ell' \gamma$ transition described by the effective Lagrangian of eq. (3.3) can generate, in addition to the anomalous magnetic moments Δa_ℓ , also lepton flavor violating (LFV) processes ($\ell \neq \ell'$), such as $\mu \rightarrow e \gamma$, and CP violating effects, such as the leptonic electric dipole moments (EDMs, d_ℓ),

$$\frac{\text{BR}(\ell \rightarrow \ell' \gamma)}{\text{BR}(\ell \rightarrow \ell' \nu_{\ell'} \bar{\nu}_{\ell'})} = \frac{48\pi^3 \alpha}{G_F^2} (|A_{\ell\ell'}|^2 + |A_{\ell'\ell}|^2), \quad \frac{d_\ell}{e} = m_\ell \text{Im}(A_{\ell\ell}). \quad (3.10)$$

Using the general parametrization for $A_{\ell\ell'}$ of eq. (3.5) we find

$$\begin{aligned} \frac{\text{BR}(\ell \rightarrow \ell' \gamma)}{\text{BR}(\ell \rightarrow \ell' \nu_{\ell'} \bar{\nu}_{\ell'})} &= \frac{48\pi\alpha G_F^{-2}}{(4\pi\Lambda_{\text{NP}})^4} \left(\left| (g_{\ell k}^L g_{\ell' k}^{L*} + g_{\ell k}^R g_{\ell' k}^{R*}) f_1(x_k) + \frac{v}{m_\ell} g_{\ell k}^L g_{\ell' k}^{R*} f_2(x_k) \right|^2 + \ell \leftrightarrow \ell' \right), \\ \frac{d_\ell}{e} &= \frac{v}{(4\pi\Lambda_{\text{NP}})^2} \text{Im}(g_{\ell k}^L g_{\ell k}^{R*}) f_2(x_k). \end{aligned} \quad (3.11)$$

On general grounds, one would expect that, in concrete NP scenarios, Δa_ℓ , d_ℓ and $\text{BR}(\ell \rightarrow \ell' \gamma)$, are correlated. In practice, their correlations depend on the unknown flavor and CP structure of the couplings g^L and g^R , and thus we cannot draw any firm conclusion. In the following, we will point out the general conditions that have to be fulfilled by any NP theory in order to account for large effects in Δa_ℓ while satisfying the constraints from d_ℓ and $\text{BR}(\ell \rightarrow \ell' \gamma)$.

Regarding the leptonic EDMs, we find the following *model-independent* relations

$$\begin{aligned} d_e &\simeq \left(\frac{\Delta a_e}{7 \times 10^{-14}} \right) 10^{-24} \tan \phi_e \quad e \text{ cm}, \\ d_\mu &\simeq \left(\frac{\Delta a_\mu}{3 \times 10^{-9}} \right) 2 \times 10^{-22} \tan \phi_\mu \quad e \text{ cm}, \\ d_\tau &\simeq \left(\frac{\Delta a_\tau}{8 \times 10^{-7}} \right) 4 \times 10^{-21} \tan \phi_\tau \quad e \text{ cm}, \end{aligned} \quad (3.12)$$

where we have defined $\phi_\ell = \arg(A_{\ell\ell})$. We have normalized Δa_μ to the central value of the current anomaly and $\Delta a_{e,\tau}$ to their values in naive scaling, $\Delta a_\ell/\Delta a_\mu = m_\ell^2/m_\mu^2$.

From eq. (3.12) we learn that an explanation of the Δa_μ anomaly implies, for a natural CPV phase $\phi_\mu \sim \mathcal{O}(1)$, a *model-independent* upper bound on $d_\mu \lesssim 3 \times 10^{-22} e \text{ cm}$ which is still far from the current bound $d_\mu \lesssim 10^{-18} e \text{ cm}$, but well within the expected future

sensitivity $d_\mu < 10^{-24} e \text{ cm}$ [61, 62]. Therefore, any experimental effort to improve the resolution on d_μ would be valuable.

On the other hand, the electron EDM imposes a bound on the corresponding CPV phase ϕ_e at the level of 10^{-3} , if NS is at work. Such a condition could be realized for instance if ϕ_e is generated radiatively while ϕ_μ arises already at the tree level. Going beyond NS, one could also envisage scenarios where the electronic dipoles are suppressed compared to the muonic dipoles because of hierarchical couplings $g_e^{L,R} \ll g_\mu^{L,R}$, as it happens for instance in a multi-Higgs doublet model where $g_\ell^{L,R}$ are related to Yukawa couplings. In general, as shown by eq. (3.11), the EDMs (but not Δa_μ) vanish if $g^L = g^R$ as it could arise in a left-right symmetric theory.

Now we discuss the potential constraints on Δa_ℓ arising from LFV processes. An inspection of eq. (3.11) shows that $\text{BR}(\ell \rightarrow \ell' \gamma)$ and Δa_ℓ are generally correlated as $\text{BR}(\ell \rightarrow \ell' \gamma) \sim (\Delta a_\mu)^2 |\theta_{\ell\ell'}|^2$ where $\theta_{\ell\ell'}$ stands for the relevant flavor mixing angle, which is approximately $\theta_{\ell\ell'} \sim \frac{g_{\ell k} g_{\ell' k}^*}{g_{\ell k} g_{\ell k}^*}$, see eq. (3.11). In particular we have

$$\begin{aligned} \text{BR}(\mu \rightarrow e \gamma) &\approx 2 \times 10^{-12} \left(\frac{\Delta a_\mu}{3 \times 10^{-9}} \right)^2 \left(\frac{\theta_{e\mu}}{3 \times 10^{-5}} \right)^2, \\ \text{BR}(\tau \rightarrow \ell \gamma) &\approx 4 \times 10^{-8} \left(\frac{\Delta a_\mu}{3 \times 10^{-9}} \right)^2 \left(\frac{\theta_{\ell\tau}}{10^{-2}} \right)^2. \end{aligned} \tag{3.13}$$

LFV contributions to Δa_ℓ can be particularly important as they are typically chirally enhanced by m_τ/m_ℓ , as we will discuss in the case of supersymmetry. Such a chiral enhancement is not effective in τ LFV processes and therefore, in this case, it might be possible to keep $\text{BR}(\tau \rightarrow \ell \gamma)$ under control, while generating large effects especially for Δa_e .

Before turning our attention to some prototype theories beyond the SM that predict non-naive scaling in Δa_ℓ , we will now briefly summarize the status of the anomalous magnetic moment of the τ .

3.3 Status of the τ anomalous magnetic moment

The present experimental sensitivity of the τ lepton $g-2$ is only 10^{-2} . In fact, while the SM prediction for a_τ is precisely known [63],

$$a_\tau^{\text{SM}} = 117\,721(5) \times 10^{-8}, \tag{3.14}$$

the very short lifetime of this lepton (2.9×10^{-13} s) makes it very difficult to determine its anomalous magnetic moment by measuring its spin precession in a magnetic field, like in the electron and muon $g-2$ experiments. Instead, experiments focused on high-precision measurements of τ pair production in various high-energy processes and comparison of the measured cross sections with the SM predictions.

The present PDG limit on the τ $g-2$ was derived by the DELPHI collaboration from $e^+e^- \rightarrow e^+e^-\tau^+\tau^-$ total cross section measurements at LEP2: $-0.052 < a_\tau^{\text{EXP}} < 0.013$ at 95% confidence level [64]. This reference also quotes the result in the form:

$$a_\tau^{\text{EXP}} = -0.018(17). \tag{3.15}$$

Comparing eqs. (3.14) and (3.15) (their difference is roughly one standard deviation), it is clear that the sensitivity of the best existing measurements is still more than an order of magnitude worse than needed. In [65], the reanalysis of various measurements of the cross section of the process $e^+e^- \rightarrow \tau^+\tau^-$, the transverse τ polarization and asymmetry at LEP and SLD, as well as of the decay width $\Gamma(W \rightarrow \tau\nu_\tau)$ at LEP and Tevatron allowed the authors to set a stronger model-independent limit on new physics contributions: $-0.007 < a_\tau^{\text{NP}} < 0.005$.

The possibility to improve these limits is certainly not excluded. Future high-luminosity B factories, such as Belle-II [66] or SuperB [67], offer new opportunities to improve the determination of the τ magnetic properties. The authors of [68, 69] proposed to measure the τ anomalous magnetic moment form factor at the Υ resonance with sensitivities down to 10^{-5} or 10^{-6} , and work is in progress for the determination of a_τ via the measurement of radiative leptonic τ decays [70–72].

4 Supersymmetry and a_e

The supersymmetric contribution to a_ℓ comes from loops with exchange of chargino/sneutrino or neutralino/charged lepton. Therefore, violations of “naive scaling” can arise through sources of non-universalities in the slepton mass matrices. Such non-universalities can be realized in two ways.

1. Lepton flavor conserving (LFC) case. The charged slepton mass matrix violates the global non-abelian flavor symmetry, but preserves $U(1)^3$. This case is characterized by non-degenerate sleptons ($m_{\tilde{e}} \neq m_{\tilde{\mu}} \neq m_{\tilde{\tau}}$) but vanishing mixing angles because of an exact alignment, which ensures that Yukawa couplings and the slepton mass matrix can be simultaneously diagonalized in the same basis.
2. Lepton flavor violating (LFV) case. The slepton mass matrix fully breaks flavor symmetry up to $U(1)$ lepton number, generating mixing angles that allow for flavor transitions. Lepton flavor violating processes, such as $\mu \rightarrow e\gamma$, provide stringent constraints on this case. However, because of flavor transitions, a_e and a_μ can receive new large contributions proportional to m_τ (from a chiral flip in the internal line of the loop diagram), giving a new source of non-naive scaling.

We will discuss these two cases separately.

4.1 Lepton flavor conserving case

In the LFC case, we assume non-degenerate slepton masses for different families ($m_{\tilde{e}} \neq m_{\tilde{\mu}} \neq m_{\tilde{\tau}}$) but flavor alignment between lepton and slepton mass matrices. This is reminiscent of the well-known alignment mechanism [73], which was proposed to solve the supersymmetric flavor problem in the quark sector by aligning the down quark/squark mass matrices and which might arise naturally in the context of abelian flavor models [74].

In this case the supersymmetric contribution to $\Delta a_\ell^{\text{LFC}}$ is given by the following approximate expression

$$\begin{aligned} \Delta a_\ell^{\text{LFC}} = & \frac{\alpha m_\ell^2}{4\pi \sin^2 \theta_W} \frac{\text{Re}(\mu M_2 \tan \beta)}{m_{\tilde{\ell}}^2(M_2^2 - \mu^2)} \left[\frac{1}{2} f_n(x_2, x_\mu) - f_c(x_2, x_\mu) \right] \\ & + \frac{\alpha m_\ell^2}{8\pi \cos^2 \theta_W} \frac{\text{Re}(\mu M_1 \tan \beta)}{m_{\tilde{\ell}}^2(M_1^2 - \mu^2)} f_n(x_1, x_\mu) \\ & - \frac{\alpha m_\ell^2}{4\pi \cos^2 \theta_W} \frac{\text{Re}(A_\ell M_1 - \mu M_1 \tan \beta)}{m_{\tilde{\ell}}^2} g_n(x_1) \quad \ell = e, \mu, \tau. \end{aligned} \quad (4.1)$$

The loop functions f_n , f_c and g_n (with $x_{1(2)} = M_{1(2)}^2/m_{\tilde{\ell}}^2$, and $x_\mu = \mu^2/m_{\tilde{\ell}}^2$) are given in the appendix, and we use standard notation for the supersymmetric parameters. In our numerical analysis we use the exact expressions for $\Delta a_\ell^{\text{LFC}}$ in the mass eigenstate basis [75].

In the illustrative case of a single mass scale ($M_{1,2} = \mu = m_{\tilde{\ell}}$) and if $\arg(\mu M_{1,2}) = \arg(A_\ell M_1) = 0$, the result simplifies to ²

$$\begin{aligned} \Delta a_\ell^{\text{LFC}} = & \frac{5\alpha_2}{48\pi} \frac{m_\ell^2}{m_{\tilde{\ell}}^2} \tan \beta + \frac{\alpha_Y}{24\pi} \frac{m_\ell^2}{m_{\tilde{\ell}}^3} A_\ell \\ \approx & 3 \times 10^{-9} \left(\frac{m_\ell}{m_\mu} \right)^2 \left(\frac{100 \text{ GeV}}{m_{\tilde{\ell}}} \right)^2 \left[\left(\frac{\tan \beta}{3} \right) + 0.1 \left(\frac{A_\ell}{3m_{\tilde{\ell}}} \right) \right]. \end{aligned} \quad (4.2)$$

This shows that the discrepancy in the muon $g-2$ can be explained by supersymmetric particles with masses around 100 (300) GeV, for $\tan \beta = 3$ (20). On the other hand, the contribution proportional to the term A_ℓ , which could induce in principle a violation of the NS if $A_e/A_\mu \neq m_e/m_\mu$, is too small to explain the muon $g-2$ anomaly after imposing the vacuum stability bound $|A_\ell|/m_{\tilde{\ell}} \lesssim 3$.

Assuming that sleptons are the heaviest particles running in the loop, we find

$$\begin{aligned} \Delta a_e \approx \Delta a_\mu \frac{m_e^2}{m_\mu^2} \frac{m_{\tilde{\mu}}^2}{m_{\tilde{e}}^2} & \approx \frac{m_{\tilde{\mu}}^2}{m_{\tilde{e}}^2} \left(\frac{\Delta a_\mu}{3 \times 10^{-9}} \right) 10^{-13}, \\ \Delta a_\tau \approx \Delta a_\mu \frac{m_\tau^2}{m_\mu^2} \frac{m_{\tilde{\mu}}^2}{m_{\tilde{\tau}}^2} & \approx \frac{m_{\tilde{\mu}}^2}{m_{\tilde{\tau}}^2} \left(\frac{\Delta a_\mu}{3 \times 10^{-9}} \right) 10^{-6}. \end{aligned} \quad (4.3)$$

For values of Δa_μ explaining the muon $g-2$, non-degenerate sleptons at the level $m_{\tilde{\mu}} \approx 3 m_{\tilde{e}}$ lead to $\Delta a_e \approx 10^{-12}$, which is at the limit of present experimental sensitivity. This naive expectation is confirmed by a complete numerical analysis, as illustrated in the left panel of figure 1, which shows Δa_e as a function of the normalized selectron/smuon mass splitting $X_{e\mu} = (m_{\tilde{e}}^2 - m_{\tilde{\mu}}^2)/(m_{\tilde{e}}^2 + m_{\tilde{\mu}}^2)$. The plot has been obtained by scanning the supersymmetric parameters that account for the $(g-2)_\mu$ anomaly at the level of $1 \leq \Delta a_\mu \times 10^9 \leq 5$ (black points), or $2 \leq \Delta a_\mu \times 10^9 \leq 4$ (red points in the inner region). We have imposed all current bounds on sparticle masses arising from direct searches and required $M_1 \leq 100$ GeV, $M_2 = 2M_1$, $\mu \leq 200$ GeV, $3 \leq \tan \beta \leq 30$, $m_{\tilde{e},\tilde{\mu}} \leq 500$ GeV. As can be clearly seen, values of Δa_e almost up to 10^{-12} are reachable for highly non-degenerate selectron and smuon masses such that $|X_{e\mu}| \sim 1$.

²The overall sign of the supersymmetric contribution to a_ℓ is a free parameter, since it is determined by $\arg(\mu M_{1,2})$, which is invariant under field phase redefinition.

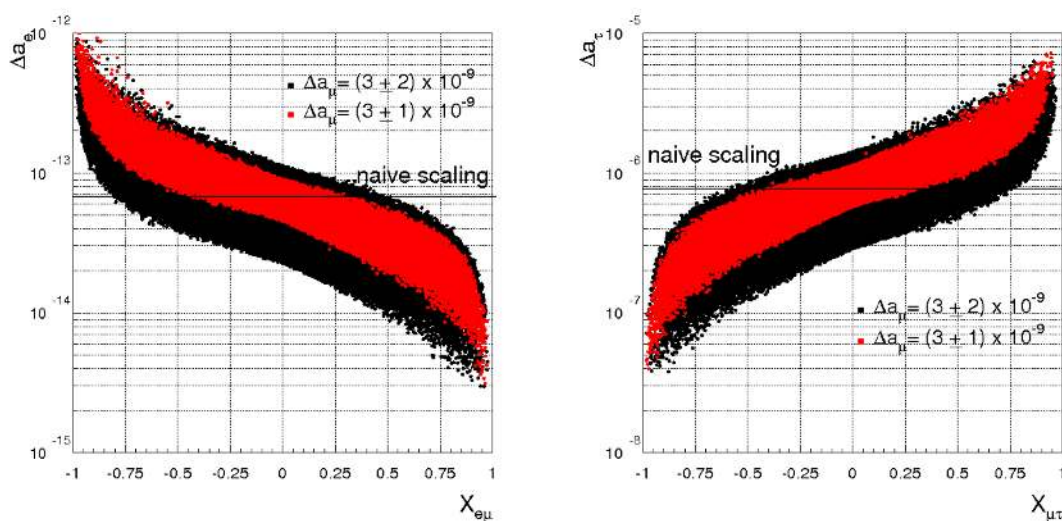


Figure 1. Left: Δa_e as a function of $X_{e\mu} = (m_{\tilde{e}}^2 - m_{\tilde{\mu}}^2)/(m_{\tilde{e}}^2 + m_{\tilde{\mu}}^2)$. Right: Δa_τ as a function of $X_{\mu\tau} = (m_{\tilde{\mu}}^2 - m_{\tilde{\tau}}^2)/(m_{\tilde{\mu}}^2 + m_{\tilde{\tau}}^2)$. Black points satisfy the condition $1 \leq \Delta a_\mu \times 10^9 \leq 5$, while red points correspond to $2 \leq \Delta a_\mu \times 10^9 \leq 4$.

In the right panel of figure 1 we show Δa_τ as a function of $X_{\mu\tau} = (m_{\tilde{\mu}}^2 - m_{\tilde{\tau}}^2)/(m_{\tilde{\mu}}^2 + m_{\tilde{\tau}}^2)$. The plot has been obtained following the same procedure described for the left panel. We observe that Δa_τ can reach the level of 10^{-5} if $m_{\tilde{\tau}} \ll m_{\tilde{\mu}}$, therefore violating NS, whose prediction is shown by the horizontal line in figure 1. The condition $m_{\tilde{\tau}} \ll m_{\tilde{\mu}}$ is justified in the so-called split family models [76, 77], where the first two generations of squarks and leptons are substantially heavier than the third generation.

Before concluding this section, it is worth to comment about the potential constraints arising from the leptonic EDMs, on the same line done in the model-independent analysis of section 3.2. From eq. (3.12) we learn that $\Delta a_e \approx 10^{-13(12)}$ is allowed only if $\arg(\mu M_{1,2}) \lesssim 10^{-3(4)}$. Moreover, since we are dealing now with *flavor-blind* CPV phases, that is $\phi = \phi_e = \phi_\mu = \phi_\tau = \arg(\mu M_{1,2})$, the electron EDM limit $d_e \lesssim 1.5 \times 10^{-27} e$ cm implies the bounds $d_\mu \lesssim 3 \times 10^{-25} e$ cm and $d_\tau \lesssim 5 \times 10^{-24} e$ cm, if $m_{\tilde{e}} \simeq m_{\tilde{\mu}} \simeq m_{\tilde{\tau}}$. Yet, values of d_μ as high as the model-independent upper bound $d_\mu \lesssim 10^{-22} e$ cm of eq. (3.12) could be reached if $m_{\tilde{e}} \gg m_{\tilde{\mu}}$, in which case the supersymmetric contributions to Δa_e and d_e could be made negligible.

4.1.1 Correlation between a_e and violation of lepton universality in LFC

In supersymmetric theories, NS violations for the leptonic $(g-2)_\ell$ can arise through sources of non-universalities in the slepton masses. In turn, these non-universalities will induce violations of lepton flavor universality in low- and high-energy processes such as $P \rightarrow \ell\nu$, $\tau \rightarrow P\nu$ (where $P = \pi, K$), $\ell_i \rightarrow \ell_j \bar{\nu}\nu$, $Z \rightarrow \ell\ell$ and $W \rightarrow \ell\nu$ through loop effects. Lepton universality has been probed at the few per-mill level so far, see table 1. It is interesting to study the correlation between such violations of lepton universality and departures from

Channel	$\Delta r^{e/\mu}$
$\Gamma(\pi \rightarrow e \bar{\nu}_e)/\Gamma(\pi \rightarrow \mu \bar{\nu}_\mu)$	-0.0045 ± 0.0032 [82, 83]
$\Gamma(K \rightarrow e \bar{\nu}_e)/\Gamma(K \rightarrow \mu \bar{\nu}_\mu)$	0.004 ± 0.004 [84]
$\Gamma(K \rightarrow \pi e \bar{\nu}_e)/\Gamma(K \rightarrow \pi \mu \bar{\nu}_\mu)$	-0.002 ± 0.004 [85]
$\Gamma(Z \rightarrow e^+ e^-)/\Gamma(Z \rightarrow \mu^+ \mu^-)$	-0.0010 ± 0.0026 [52, 86–89]
$\Gamma(W \rightarrow e \bar{\nu}_e)/\Gamma(W \rightarrow \mu \bar{\nu}_\mu)$	0.017 ± 0.019 [52, 86–89]
$\Gamma(\tau \rightarrow \nu_\tau e \bar{\nu}_e)/\Gamma(\tau \rightarrow \nu_\tau \mu \bar{\nu}_\mu)$	-0.0036 ± 0.0028 [90]
Channel	$\Delta r^{\mu/\tau}$
$\Gamma(\pi \rightarrow \mu \bar{\nu}_\mu)/\Gamma(\tau \rightarrow \pi \nu_\tau)$	0.016 ± 0.008
$\Gamma(K \rightarrow \mu \bar{\nu}_\mu)/\Gamma(\tau \rightarrow K \nu_\tau)$	0.037 ± 0.016 [90]
$\Gamma(Z \rightarrow \mu^+ \mu^-)/\Gamma(Z \rightarrow \tau^+ \tau^-)$	-0.0011 ± 0.0034 [52, 86–89]
$\Gamma(W \rightarrow \mu \bar{\nu}_\mu)/\Gamma(W \rightarrow \tau \bar{\nu}_\tau)$	-0.060 ± 0.021 [52, 86–89]
$\Gamma(\mu \rightarrow \nu_\mu e \bar{\nu}_e)/\Gamma(\tau \rightarrow \nu_\tau e \bar{\nu}_e)$	-0.0014 ± 0.0044 [90]
Channel	$\Delta r^{e/\tau}$
$\Gamma(Z \rightarrow e^+ e^-)/\Gamma(Z \rightarrow \tau^+ \tau^-)$	-0.0020 ± 0.0030 [52, 86–89]
$\Gamma(W \rightarrow e \bar{\nu}_e)/\Gamma(W \rightarrow \tau \bar{\nu}_\tau)$	-0.044 ± 0.021 [52, 86–89]
$\Gamma(\mu \rightarrow \nu_\mu e \bar{\nu}_e)/\Gamma(\tau \rightarrow \nu_\tau \mu \bar{\nu}_\mu)$	-0.0032 ± 0.0042 [90]

Table 1. Experimental limits on $\Delta r^{\ell/\ell'}$ with $\ell, \ell' = e, \mu, \tau$.

NS for Δa_ℓ . Taking for example the process $P \rightarrow \ell \nu$, we can define the quantity

$$\frac{(R_P^{e/\mu})_{\text{EXP}}}{(R_P^{e/\mu})_{\text{SM}}} = 1 + \Delta r_P^{e/\mu}. \quad (4.4)$$

Here $(R_P^{e/\mu})_{\text{SM}} = \Gamma(P \rightarrow e \nu)_{\text{SM}}/\Gamma(P \rightarrow \mu \nu)_{\text{SM}}$ and $(R_P^{e/\mu})_{\text{EXP}} = \Gamma(P \rightarrow e \nu)_{\text{EXP}}/\Gamma(P \rightarrow \mu \nu)_{\text{EXP}}$ so that $\Delta r_P^{e/\mu} \neq 0$ signals the presence of new physics violating lepton universality.

Within supersymmetry, in the absence of LFV sources, $\Delta r_P^{e/\mu}$ is induced at the loop level by box, wave function renormalization and vertex contributions from sparticle exchange. The complete calculation of μ decay in supersymmetry [78–81] can be easily applied to meson decays and we have included the full result in our numerical analysis. Neglecting box contributions, which are suppressed by heavy squark masses, the parametrical structure of $\Delta r_P^{e/\mu}$ is

$$\Delta r_P^{e/\mu} \sim \frac{\alpha}{4\pi} \left(\frac{m_{\tilde{e}}^2 - m_{\tilde{\mu}}^2}{m_{\tilde{e}}^2 + m_{\tilde{\mu}}^2} \right) \frac{v^2}{\min(m_{\tilde{e}, \tilde{\mu}}^2)}, \quad (4.5)$$

where the term $v^2/\min(m_{\tilde{e}, \tilde{\mu}}^2)$ stems from SU(2) breaking effects.

Within supersymmetry, such SU(2) breaking sources arise from left-right soft breaking terms, from mixing terms in the chargino/neutralino mass matrices, or from D-terms.

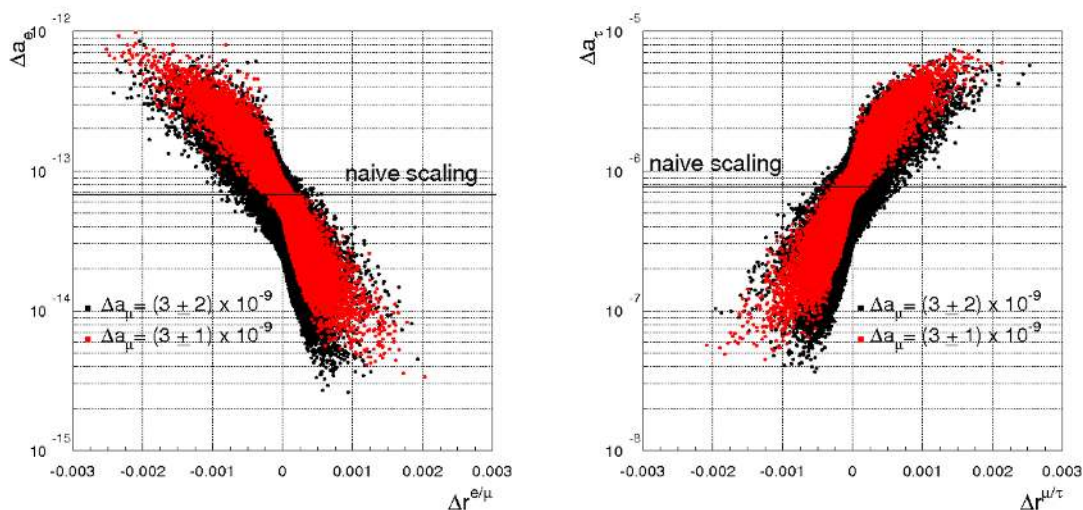


Figure 2. Left: $\Delta r_P^{e/\mu}$ as a function of Δa_e , where $\Delta r_P^{e/\mu}$ measures violations of lepton universality in $\Gamma(P \rightarrow e\nu)/\Gamma(P \rightarrow \mu\nu)$ with $P = K, \pi$. Right: $\Delta r_P^{\mu/\tau}$ as a function of Δa_τ where $\Delta r_P^{\mu/\tau}$ measures violations of lepton universality in $\Gamma(P \rightarrow \mu\nu)/\Gamma(\tau \rightarrow P\nu)$ with $P = K, \pi$. Black points satisfy the condition $1 \leq \Delta a_\mu \times 10^9 \leq 5$, while red points correspond to $2 \leq \Delta a_\mu \times 10^9 \leq 4$.

For highly non degenerate sleptons and if $\min(m_{\tilde{e},\tilde{\mu}}^2) \sim v^2$, $\Delta r_P^{e/\mu}$ can reach the few per-mill level.

Given that the NP sensitivity of $\pi \rightarrow \ell\nu$ and $K \rightarrow \ell\nu$ to the above effects is the same, and that their present experimental resolutions are comparable, both $\pi \rightarrow \ell\nu$ and $K \rightarrow \ell\nu$ represent useful probes of this scenario. Future experiments at TRIUMF and PSI aim at testing lepton universality in $\pi \rightarrow \ell\nu$ at the level of $< 1 \times 10^{-3}$ and 5×10^{-4} , respectively. Both the NA62 experiment at CERN and the KLOE-2 experiment will continue improving their sensitivity aiming at a test of lepton universality in $K \rightarrow \ell\nu$ at the few per-mill level.

In figure 2, on the left, which has been obtained through the same scanning procedure described for figure 1, we show the quantity $\Delta r_{K,\pi}^{e/\mu}$, defined in eq. (4.4), as a function of Δa_e . We learn that large NS violations typically imply also breaking effects of lepton universality at the few per-mill level, which are expected to be within the future experimental reach.

Similarly, in figure 2, on the right, we show breaking effects of lepton universality in the μ/τ sector, accounted for by the quantity $\Delta r_{K,\pi}^{\mu/\tau}$ which can be constructed for instance combining processes like $\tau \rightarrow P\nu$ and $P \rightarrow \mu\nu$ (where $P = \pi, K$). Large NS violations, bringing Δa_τ to the level of 10^{-5} , are typically correlated with violations of lepton universality in the μ/τ sector at the per-mill level. These effects will be tested experimentally at the SuperB, which aims at LFU tests in τ decays well below the per-mill level [91].

4.2 Lepton flavor violating case

We now consider LFV contributions to a_ℓ . The importance of this case lies in the fact that LFV can generate contributions to a_e and a_μ that are chirally enhanced, being proportional to m_τ [120, 121]. Using the mass-insertion approximation, which is valid for near degenerate

BR($\mu^- \rightarrow e^- \gamma$) < 2.4×10^{-12} [92]
BR($\tau^- \rightarrow \mu^- \gamma$) < 4.4×10^{-8} [93–108]
BR($\tau^- \rightarrow e^- \gamma$) < 3.3×10^{-8} [93–108]

Table 2. 90% C.L. limits on radiative LFV decays.

sleptons with mass $m_{\tilde{\ell}}$, we find

$$\Delta a_{\ell}^{\text{LFV}} \simeq \frac{\alpha_1}{\pi} \left(\frac{m_{\ell} m_{\tau}}{m_{\tilde{\ell}}^2} \right) \tan \beta \frac{\text{Re}(\mu M_1 \delta_{RR}^{\ell\tau} \delta_{LL}^{\tau\ell})}{m_{\tilde{\ell}}^2} l_n(x_1) \quad \ell = e, \mu. \quad (4.6)$$

We defined $\delta_{AB}^{ij} = (m_{AB}^2)^{ij}/m_{\tilde{\ell}}^2$ (with $A, B = L, R$), where m_{LL}^2 and m_{RR}^2 stand for the left- and right-handed slepton mass square matrices. The function l_n is given in the appendix. In the illustrative case where $m_{\tilde{\ell}} = M_1$, we find

$$\Delta a_{\ell}^{\text{LFV}} \approx 5 \times 10^{-13} \left(\frac{m_{\ell}}{m_e} \right) \left(\frac{\tan \beta}{30} \right) \left(\frac{2 \text{ TeV}}{m_{\tilde{\ell}}} \right)^2 \left(\frac{\mu/m_{\tilde{\ell}}}{2} \right) \left(\frac{\delta_{RR}^{\ell\tau}}{0.5} \right) \left(\frac{\delta_{LL}^{\tau\ell}}{0.5} \right) \quad \ell = e, \mu. \quad (4.7)$$

As evident from eq. (4.6), the single power of m_{ℓ} and the flavor mixing angles of the soft sector break NS and provide a potentially large chiral enhancement $m_{\tau}/m_{e,\mu}$, which is especially important for Δa_e [121].

4.2.1 Correlation between a_e and $\tau \rightarrow e\gamma$ in LFV

The case of LFV has to be confronted with the strong constraints from processes like $l_i \rightarrow l_j \gamma$, see table 2. The decay rate of $l_i \rightarrow l_j \gamma$ is given by

$$\frac{\text{BR}(l_i \rightarrow l_j \gamma)}{\text{BR}(l_i \rightarrow l_j \nu_i \bar{\nu}_j)} = \frac{48\pi^3 \alpha}{G_F^2} \left(|A_L^{ij}|^2 + |A_R^{ij}|^2 \right). \quad (4.8)$$

The supersymmetric contributions to $\mu \rightarrow e\gamma$ and $\tau \rightarrow l\gamma$ ($\ell = e, \mu$) amplitudes arise at one loop level through the exchange of charginos/sneutrinos and neutralinos/sleptons. Although our numerical results are based on the exact expressions for $A_{L,R}^{ij}$ in the mass eigenstate basis [109], in the following we provide their expressions in the mass-insertion approximation [110]

$$\begin{aligned} A_L^{ij} \simeq & \frac{\alpha}{4\pi \sin^2 \theta_W} \frac{\delta_{LL}^{ij}}{m_{\tilde{\ell}}^2} \frac{\mu M_2 \tan \beta}{(M_2^2 - \mu^2)} \left[g_n(x_2, x_{\mu}) + g_c(x_2, x_{\mu}) \right] \\ & + \frac{\alpha}{4\pi \cos^2 \theta_W} \frac{\delta_{LL}^{ij}}{m_{\tilde{\ell}}^2} \mu M_1 \tan \beta \left[\frac{h_n(x_1)}{m_{\tilde{\ell}}^2} - \frac{g_n(x_1, x_{\mu})}{(M_1^2 - \mu^2)} \right] \\ & + \frac{\alpha}{4\pi \cos^2 \theta_W} \frac{\delta_{RL}^{ij}}{m_{\tilde{\ell}}^2} \left(\frac{M_1}{m_{\ell_i}} \right) 2f_n(x_1), \end{aligned} \quad (4.9)$$

$$A_R^{ij} \simeq \frac{\alpha}{4\pi \cos^2 \theta_W} \left[\frac{\delta_{RR}^{ij}}{m_{\tilde{\ell}}^2} \mu M_1 \tan \beta \left(\frac{h_n(x_1)}{m_{\tilde{\ell}}^2} + \frac{2g_n(x_1, x_{\mu})}{(M_1^2 - \mu^2)} \right) + \frac{\delta_{LR}^{ij}}{m_{\tilde{\ell}}^2} \left(\frac{M_1}{m_{\ell_i}} \right) 2f_n(x_1) \right]. \quad (4.10)$$

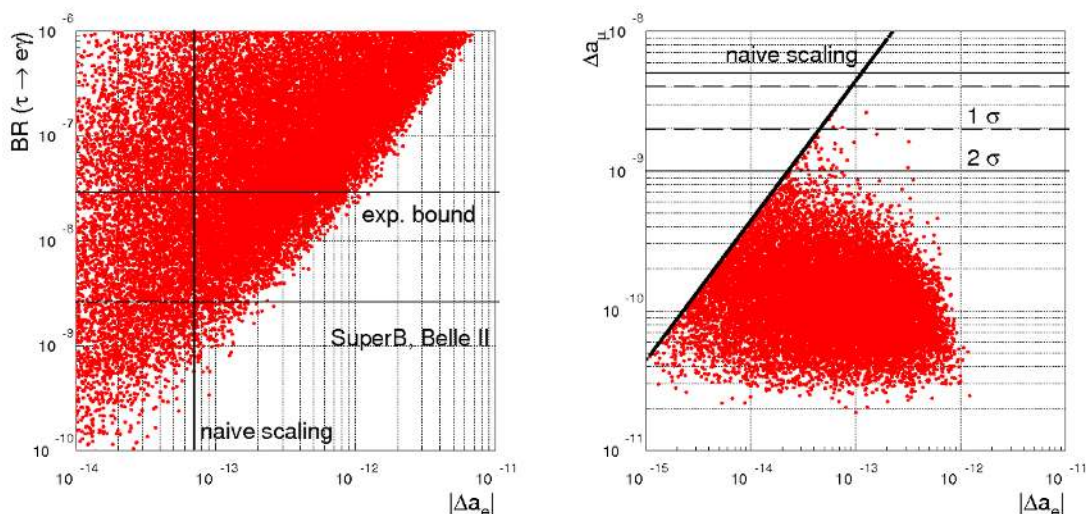


Figure 3. Left: $\text{BR}(\tau \rightarrow e\gamma)$ vs. $|\Delta a_e|$ in the LFV scenario. The horizontal lines show the current bound and the expected future experimental sensitivity on $\text{BR}(\tau \rightarrow e\gamma)$. The vertical line corresponds to the prediction for Δa_e assuming a NS setting Δa_μ to its central value $\Delta a_\mu = 3 \times 10^{-9}$. Right: Δa_μ vs. $|\Delta a_e|$ in the LFV scenario imposing the bound $\text{BR}(\tau \rightarrow e\gamma) < 3.3 \times 10^{-8}$. The black line shows the correlation between Δa_μ and Δa_e in the case of naive scaling. The horizontal dashed (solid) lines show the 1σ (2σ) Δa_μ anomaly $\Delta a_\mu \approx (3 \pm 1) \times 10^{-9}$, see eq. (1.1).

In the region of parameter space that maximizes Δa_e , corresponding to moderate/large $\tan\beta$ values and a large μ term, $\text{BR}(\tau \rightarrow \ell\gamma)$ can be approximated as

$$\text{BR}(\tau \rightarrow \ell\gamma) \approx 3 \times 10^{-8} \left(\frac{\tan\beta}{30} \right)^2 \left(\frac{2\text{TeV}}{m_{\tilde{\ell}}} \right)^4 \left(\frac{\mu/m_{\tilde{\ell}}}{2} \right)^2 \left(\left| \frac{\delta_{LL}^{\tau\ell}}{0.5} \right|^2 + \left| \frac{\delta_{RR}^{\tau\ell}}{0.5} \right|^2 \right). \quad (4.11)$$

Combining eq. (4.11) with eq. (4.7), one can set an upper bound on Δa_ℓ as a function of $\text{BR}(\tau \rightarrow \ell\gamma)$. We have studied this correlation numerically and we show in figure 3 our results for Δa_e vs. $\text{BR}(\tau \rightarrow e\gamma)$. The plot has been obtained by means of a scan with $M_1 \leq 2\text{TeV}$, $M_2 = 2M_1$, $\mu \leq 5\text{TeV}$, $3 \leq \tan\beta \leq 30$, $m_{\tilde{\ell}} \leq 2\text{TeV}$, $|\delta_{RR}^{\tau e}| < 1$, $|\delta_{LL}^{\tau e}| < 1$. As illustrated in figure 3, the experimental limit $\text{BR}(\tau \rightarrow e\gamma) < 3.3 \times 10^{-8}$ (90% CL) curiously corresponds to a limit on Δa_e close to 10^{-12} , which is just at the edge of present experimental sensitivity. Therefore, in the case of LFV, any future positive indication for Δa_e will necessarily imply that $\tau \rightarrow e\gamma$ is just beyond the present bound. Moreover, even if $\tau \rightarrow e\gamma$ will not be detected at the upcoming SuperB and Belle II facilities, which are expected to reach the sensitivity of $\text{BR}(\tau \rightarrow e\gamma) \lesssim 3 \times 10^{-9}$, we can still expect values for Δa_e up to the level of $\Delta a_e \lesssim 2 \times 10^{-13}$, which is roughly a factor of three above the expectations of the NS scenario.

However, in contrast to the LFC scenario, LFV is not able to account for the Δa_μ anomaly, with departure from NS. This is because by combining eq. (4.11) with eq. (4.7) we find that the experimental limit $\text{BR}(\tau \rightarrow \mu\gamma) < 4.4 \times 10^{-8}$ (90% CL) sets a very strong upper bound on $\Delta a_\mu^{\text{LFV}}$. Moreover, large effects in $\Delta a_\mu^{\text{LFV}}$ require slepton masses roughly at

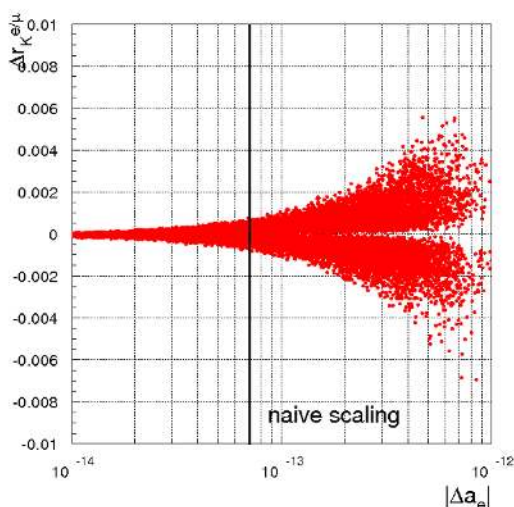


Figure 4. $\Delta r_K^{e/\mu}$ vs. $|\Delta a_e|$ in the LFV scenario. The vertical line corresponds to the prediction for Δa_e assuming NS, setting Δa_μ equal to its central value $\Delta a_\mu = 3 \times 10^{-9}$.

the TeV, in order to keep $\text{BR}(\tau \rightarrow e\gamma)$ under control. In such a regime, we cannot employ the contribution to $(g-2)_\mu$ from LFC because $\Delta a_\mu^{\text{LFC}}$ is not large enough in order to account for the anomaly, see eq. (4.2). This can be clearly seen in figure 3 on the right where we show Δa_μ vs. $|\Delta a_e|$ in the LFV scenario, imposing the bound $\text{BR}(\tau \rightarrow e\gamma) < 3.3 \times 10^{-8}$. The black line shows the correlation between Δa_μ and Δa_e in the case of NS where LFV contributions are absent. In the interesting region where $10^{-13} \lesssim \Delta a_e \lesssim 10^{-12}$, it turns out that Δa_μ is below the level of 10^{-9} .

Finally, there is a formidable constraint from $\mu \rightarrow e\gamma$, a process that receives contributions from the combination of flavor mixing angles $\delta_{\mu e} \approx \delta^{\mu\tau} \delta^{\tau e}$. Therefore, in order to fulfill the $\text{BR}(\mu \rightarrow e\gamma)$ bound while generating sizable effects for $\Delta a_e \propto \delta^{e\tau} \delta^{\tau e}$, we need a strong hierarchy such that $\delta_{AB}^{\mu\tau} \ll \delta_{AB}^{e\tau}$. In conclusion, a large contribution to Δa_e in the LFV case is possible if the only sizable mixing is between the first and third generation of sleptons.

Also in the LFV case a potential constraint can arise from the leptonic EDMs. In particular, in order to obtain $\Delta a_e \approx 10^{-13(12)}$ we need a suppression for the relevant CPV phase $\arg(\mu M_1 \delta_{RR}^{\ell\tau} \delta_{LL}^{\tau\ell}) \lesssim 10^{-3(4)}$. However, in contrast with the LFC case, we have now *flavor-dependent* CPV phases and therefore the electron EDM does not constrain directly $d_{\mu,\tau}$. Still, whenever $d_{\mu,\tau}$ are induced by *flavor-dependent* phases (coming from LFV sources), powerful bounds are obtained by the LFV processes $\ell_i \rightarrow \ell_j \gamma$. In particular, we find that the current bound $\text{BR}(\tau \rightarrow \mu\gamma) < 4.4 \times 10^{-8}$ sets the upper bounds $d_\mu \lesssim 3 \times 10^{-23} e \text{ cm}$ and $d_\tau \lesssim 1.5 \times 10^{-24} e \text{ cm}$.

4.2.2 Correlation between a_e and violation of lepton universality in LFV

Violations of lepton universality can arise also in the LFV scenario. The quantity that is determined experimentally and accounts for deviations from μ - e universality is

$$\left(R_P^{e/\mu}\right)_{\text{EXP}} = \frac{\sum_i \Gamma(P \rightarrow e\nu_i)}{\sum_i \Gamma(P \rightarrow \mu\nu_i)} \quad i = e, \mu, \tau. \quad (4.12)$$

The sums extend over all neutrino (or antineutrino) flavors since they cannot be distinguished experimentally. This is important for our purposes because in the LFV case one expects new contributions to $P \rightarrow e\nu_\tau$, a process that is detected as breaking of lepton universality, rather than violation of lepton flavor.

One would naively expect that the LFV channels $P \rightarrow \ell_i\nu_k$ ($i \neq k$) are suppressed compared with the LFC ones ($i = k$). An interesting exception is provided by charged Higgs mediated LFV contributions, which can be sizable for large $\tan\beta$ and which are chirally-enhanced by the factor m_τ/m_ℓ [111, 112]. Indeed, the dominant contribution to $\Delta r_P^{e/\mu}$ in the case of mixing between the first and third generation sleptons is

$$1 + \Delta r_P^{e/\mu} \simeq \left| 1 - \frac{m_P^2}{M_{H^\pm}^2} \frac{m_\tau}{m_e} \Delta_{RL}^{11} \tan^3 \beta \right|^2 + \left(\frac{m_P^4}{M_{H^\pm}^4} \right) \left(\frac{m_\tau^2}{m_e^2} \right) |\Delta_{RR}^{31}|^2 \tan^6 \beta. \quad (4.13)$$

The coefficients Δ_{RL}^{11} and Δ_{RR}^{31} measure the effective couplings $H^+\bar{\nu}_{eL}e_R$ and $H^+\bar{\nu}_{\tau L}e_R$ respectively, which are induced at one-loop level by exchange of Bino or Bino-Higgsino and sleptons. Since these effective Yukawa interactions are of dimension four, the quantities Δ_{RL}^{11} and Δ_{RR}^{31} are not sensitive to the overall soft scale, hence avoiding supersymmetric decoupling. In the region of parameter space where Δa_e receives large effects, i.e. for $\mu \gg m_{\tilde{\ell}} \sim M_1$, it turns out that³

$$\Delta r_P^{e/\mu} \approx 8 \times 10^{-3} \left(\frac{0.5 \text{ TeV}}{M_{H^\pm}} \right)^2 \left(\frac{\mu/m_{\tilde{\ell}}}{2} \right) \left(\frac{\delta_{LL}^{e\tau}}{0.5} \right) \left(\frac{\delta_{RR}^{\tau e}}{0.5} \right) \left(\frac{\tan\beta}{30} \right)^3. \quad (4.14)$$

An inspection of eqs. (4.6), (4.14) reveals that LFV effects contributing to $\Delta a_\ell^{\text{LFV}}$ and $\Delta r_K^{e/\mu}$ are correlated, as shown in figure 4. The plot has been obtained by means of a scan with $10 \leq \tan\beta \leq 50$, $M_{H^\pm} \leq 1 \text{ TeV}$, $M_1 \leq 2 \text{ TeV}$, $M_2 = 2M_1$, $\mu \leq 5 \text{ TeV}$, $m_{\tilde{\ell}} \leq 2 \text{ TeV}$, and $|\delta_{AB}^{\tau e}| < 1$. It is interesting that $\Delta a_\ell^{\text{LFV}}$ and $\Delta r_K^{e/\mu}$ can simultaneously reach experimentally testable values even for supersymmetric masses beyond the LHC reach.

Turning to pion physics, one finds that $\Delta r_\pi^{e/\mu} \sim (m_\pi^2/m_k^2) \times \Delta r_K^{e/\mu}$. Therefore $\Delta r_{\pi}^{e/\mu}{}_{\text{susy}}$ is negligible after the constraints from $\Delta r_K^{e/\mu}{}_{\text{susy}}$ are imposed.

4.3 Disoriented A-terms

So far, we have investigated various supersymmetric scenarios and their capability to account for the muon $g-2$ anomaly. In particular, we have analyzed the possibility of breaking

³In particular, starting from the exact expressions for Δ_{RR}^{31} and Δ_{RL}^{11} in the mass eigenstate basis [113, 114], which we use in our numerical analysis, one can find that $\Delta_{RR}^{31} \simeq \frac{\alpha_1}{16\pi} \frac{\mu}{m_{\tilde{\ell}}} \delta_{RR}^{\tau e}$ and $\Delta_{RL}^{11} \simeq -\frac{\alpha_1}{32\pi} \frac{\mu}{m_{\tilde{\ell}}} \delta_{LL}^{e\tau} \delta_{RR}^{\tau e}$ for $\mu \gg m_{\tilde{\ell}} \sim M_1$. Notice that $\text{Im}(\delta_{LL}^{e\tau} \delta_{RR}^{\tau e})$ is strongly constrained by the electron EDM. However, sizable contributions to $\Delta r_P^{e/\mu}$ can still be induced by $\text{Re}(\delta_{LL}^{e\tau} \delta_{RR}^{\tau e})$.

the NS among different leptonic $g-2$. As discussed in the previous sections, both model-independently as well as in supersymmetric frameworks, the major challenge we have to deal with, when generating large effects for the leptonic $g-2$, is to keep under control other dipole transitions like the electron EDM and $\mu \rightarrow e\gamma$. Yet, the correlation among Δa_ℓ , d_ℓ and $\text{BR}(\ell \rightarrow \ell'\gamma)$ depends on the unknown flavor and CP structure of new physics. Therefore, from a phenomenological perspective, d_ℓ and $\text{BR}(\ell \rightarrow \ell'\gamma)$ do not provide a direct bound on new contributions to Δa_ℓ .

However, it would be desirable to have a concrete scenario where the above conditions are naturally fulfilled. In the following, we point out that this happens in the case of the so-called “disoriented A-terms”, invoked in ref. [115] to account for the recently observed direct CP violation in charm decays $D \rightarrow KK, \pi\pi$.

The assumption of disoriented A-terms is that flavor violation is restricted to the trilinear terms

$$(\delta_{LR}^{ij})_f \sim \frac{A_f \theta_{ij}^f m_{f_j}}{m_{\tilde{f}}} \quad f = u, d, \ell, \quad (4.15)$$

where θ_{ij}^f are generic mixing angles. This pattern can be obtained when the trilinear terms have the same hierarchical pattern as the corresponding Yukawa matrices but they do not respect exact proportionality. A natural realization of this ansatz arises in scenarios with partial compositeness, as recently pointed out in ref. [116]. Interestingly, the structure of eq. (4.15) allows us to naturally satisfy the very stringent flavor bounds of the down-sector thanks to the smallness of down-type quark masses. Similarly, also the bounds from the lepton sector can be satisfied under the (natural) assumption that the unknown leptonic flavor mixing angles are of the form $\theta_{ij}^\ell \sim \sqrt{m_i/m_j}$ [116].

In the disoriented A-term scenario, the dominant amplitude for $\mu \rightarrow e\gamma$ is

$$A_L^{\mu e} = \frac{\alpha M_1 \delta_{LR}^{\mu e}}{2\pi \cos^2 \theta_W m_{\tilde{\ell}}^2 m_\mu} f_n(x_1), \quad (4.16)$$

where $x_1 = M_1^2/m_{\tilde{\ell}}^2$. Assuming that the only possible sources of CP violation arise from A terms, the electron EDM d_e is generated by the one-loop exchange of Bino and charged sleptons. One can find the following approximate expression

$$\frac{d_e}{e} = \frac{\alpha \text{Im}(M_1 \delta_{LR}^{ee})}{2\pi \cos^2 \theta_W \tilde{m}^2} f_n(x_1). \quad (4.17)$$

On the other hand, the $g-2$ does not require any source of CP violation and therefore it always receives effects also from SU(2) interactions. In particular, the leading effects is

$$\Delta a_\ell \simeq \frac{\alpha m_\ell^2 \tan \beta}{\pi \sin^2 \theta_W \tilde{m}^2} f'(x_2), \quad (4.18)$$

where we have considered the illustrative case where $M_2 = \mu$, so that $x_2 = M_2^2/\tilde{m}^2 = \mu^2/\tilde{m}^2$. The loop function is such that $f'(1) = 1/8$ and $f'(0) = 1/2$.

Therefore, the leading SUSY contribution for $g-2$ is parametrically enhanced relatively to the amplitude generating d_e and $\mu \rightarrow e\gamma$ by a factor of $\sim \tan \beta / \tan^2 \theta_W \approx 100 \times$

$(\tan \beta/30)$. This naturally raises the question of whether it is possible to account for the $(g-2)_\mu$ anomaly, while satisfying in a natural way the constraints from d_e and $\mu \rightarrow e\gamma$. Indeed, the latter constraints generally require slepton masses around the TeV scale, if we assume $A \sim \tilde{m}$ with $\mathcal{O}(1)$ phases and $\theta_{ij}^\ell \sim \sqrt{m_i/m_j}$. Even with such large slepton masses, it is still possible to account for the $(g-2)_\mu$ anomaly if gauginos are significantly lighter than sleptons, which is also welcome from naturalness arguments. This can be seen observing that if $x_2 \ll 1$, that is if $M_2, \mu \ll \tilde{m}$, the relevant loop function for Δa_μ is enhanced by a factor of four compared to the case where $M_2 = \mu = \tilde{m}$. At the same time, both $\text{BR}(\mu \rightarrow e\gamma)$ and d_e tend to decrease when $M_1 \ll \tilde{m}$, see eqs. (4.16), (4.17). Clearly, one could equivalently consider a lighter supersymmetric spectrum to explain the muon $g-2$ and A_ℓ terms somewhat smaller than \tilde{m} .

In particular, setting $\tilde{m} = |A_e| = 1$ TeV, $\sin \phi_{A_e} = 1$, $M_2 = \mu = 2M_1 = 0.2$ TeV, and $\tan \beta = 30$, we find that

$$\begin{aligned} \text{BR}(\mu \rightarrow e\gamma) &\approx 6 \times 10^{-13} \left| \frac{A_\ell}{\text{TeV}} \frac{\theta_{12}^\ell}{\sqrt{m_e/m_\mu}} \right|^2 \left(\frac{\text{TeV}}{m_{\tilde{\ell}}} \right)^4, \\ d_e &\approx 4 \times 10^{-28} \text{Im} \left(\frac{A_\ell \theta_{11}^\ell}{\text{TeV}} \right) \left(\frac{\text{TeV}}{m_{\tilde{\ell}}} \right)^2 e \text{ cm}, \\ \Delta a_\mu &\approx 1 \times 10^{-9} \left(\frac{\text{TeV}}{m_{\tilde{\ell}}} \right)^2 \left(\frac{\tan \beta}{30} \right). \end{aligned} \tag{4.19}$$

These estimates are fully confirmed by the numerical analysis shown in figure 5 which has been obtained by means of the following scan: $0.5 \leq |A_e|/\tilde{m} \leq 2$ with $\sin \phi_{A_e} = 1$, $\tilde{m} \leq 2$ TeV, $(M_2, \mu, M_1) \leq 1$ TeV and $10 \leq \tan \beta \leq 50$.

It is interesting that disoriented A-terms can account for $(g-2)_\mu$, satisfy the bounds on $\mu \rightarrow e\gamma$ and d_e , while giving predictions within experimental reach. However, we expect that the electron $g-2$ follows NS. A potential source of NS breaking comes from the trilinear terms (provided $A_e/A_\mu \neq m_e/m_\mu$). In practice, as already discussed in previous sections, their effects are very small after the vacuum stability bound $|A_\ell|/m_\ell \lesssim 3$ are imposed and therefore the NS relations are preserved.

5 Light (pseudo)scalars and a_e

In this section we will investigate scenarios where the muon $g-2$ anomaly is accounted for by contributions arising from light (pseudo)scalar particles.⁴ Irrespectively of the underlying theoretical motivations, such framework is interesting because it typically predicts large and very special NS violations.

We parametrize the Yukawa interactions between the light scalar field ϕ and pseudoscalar A with leptons ℓ with the following effective Lagrangian

$$\mathcal{L} = \left(\frac{gm_\ell}{2M_W} \right) C_\phi^\ell \bar{\ell}\ell\phi + i \left(\frac{gm_\ell}{2M_W} \right) C_A^\ell \bar{\ell}\gamma_5\ell A, \tag{5.1}$$

⁴The relevance of light vector boson contributions to the muon and electron $g-2$ has been recently discussed in [122, 123].

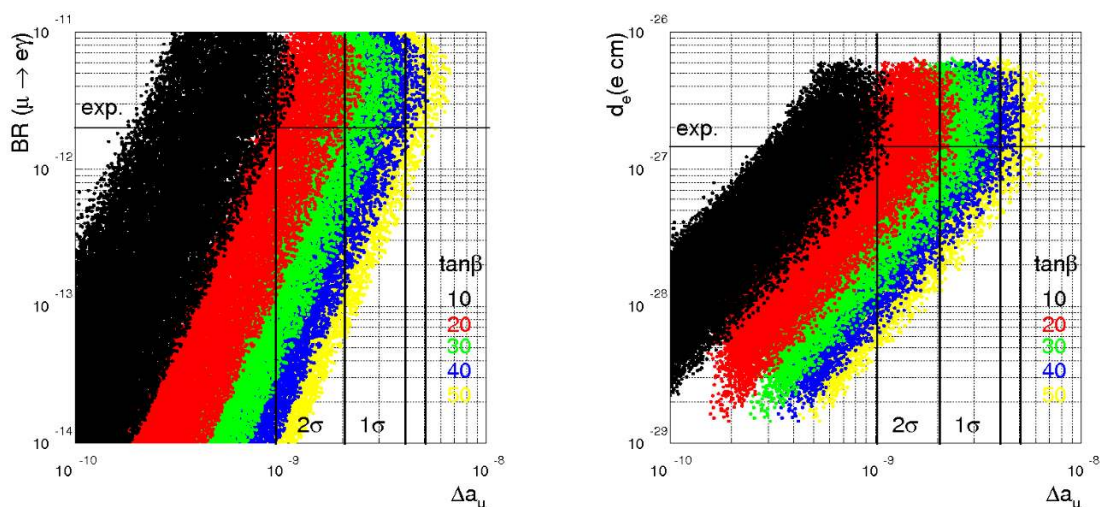


Figure 5. Predictions for $\mu \rightarrow e\gamma$, Δa_μ and d_e in the disoriented A-term scenario [115] assuming $\theta_{ij}^\ell = \sqrt{m_i/m_j}$. Left: $\mu \rightarrow e\gamma$ vs. Δa_μ . Right: d_e vs. Δa_μ .

where C_ϕ^ℓ and C_A^ℓ are arbitrary constants. Although we will not discuss specific models, the field A could arise as a pseudo-Goldstone boson of an extended Higgs sector and the field ϕ could be a light gauge singlet coupled through a dimension-five effective interaction to the ordinary Yukawa terms.

Very light scalar or pseudoscalar particles with Yukawa-like couplings are generally subject to stringent constraints both from low-energy data, such as meson decays, as well as reactor and beam dump experiments (for a review see ref. [117]). Most of these bounds disappear for $M_A \gtrsim 10$ GeV, which is the mass regime of interest for us in order to account for the $(g-2)_\mu$ anomaly, as we will show below. For simplicity, we can also consider the case in which ϕ and A are coupled to leptons, but not to quarks. Because of the smallness of the electron Yukawa coupling, this case is even less constrained.

5.1 One-loop effects

The one-loop contribution due to (pseudo)scalar particles to $(g-2)_\ell$ is [118],

$$(\Delta a_\ell^{\phi A})_{1\text{loop}} = \frac{g^2 m_\ell^4}{32\pi^2 M_W^2} \left(|C_\phi^\ell|^2 \frac{I_\phi^\ell}{M_\phi^2} - |C_A^\ell|^2 \frac{I_A^\ell}{M_A^2} \right), \quad (5.2)$$

where the loop functions $I_{\phi,A}$ are

$$I_\phi^\ell = \int_0^1 dz \frac{z^2(2-z)}{1-z+z^2 r_\phi^\ell}, \quad I_A^\ell = \int_0^1 dz \frac{z^3}{1-z+z^2 r_A^\ell}, \quad (5.3)$$

with $r_{\phi,A}^\ell = m_\ell^2/M_{\phi,A}^2$ and with asymptotic limits

$$I_\phi^\ell = \begin{cases} \frac{3}{2r} & r \gg 1 \\ -\ln r - \frac{7}{6} & r \ll 1 \end{cases}, \quad I_A^\ell = \begin{cases} \frac{1}{2r} & r \gg 1 \\ -\ln r - \frac{11}{6} & r \ll 1 \end{cases}. \quad (5.4)$$

Note that the one-loop pseudoscalar (scalar) effect is unambiguously negative (positive). Therefore, at this level, a light pseudoscalar particle cannot explain the muon $g-2$ anomaly as it contributes to Δa_μ with the wrong sign. Moreover, for $m_\ell \gg M_{\phi,A}$ we find NS, $\Delta a_\ell \propto m_\ell^2$, see eqs. (5.2), (5.4). On the other hand, in the opposite limit $m_\ell \ll M_{\phi,A}$, Δa_ℓ roughly scales with the fourth power of lepton masses (apart from a mild logarithmic dependence) $\Delta a_\ell \propto m_\ell^4 \ln(M_{\phi,A}/m_\ell)$, see eq. (5.4).

5.2 Two-loop effects

Since in the $m_\ell \ll M_{\phi,A}$ regime the one loop contributions to Δa_ℓ are highly suppressed by the fourth power of lepton masses, two loop effects might be relevant whenever we can avoid large powers of light lepton masses. This is indeed the case for two-loop Barr-Zee type diagrams with an effective $A\gamma\gamma$ vertex generated by the exchange of heavy fermions. Here we consider only the effect of the τ lepton, but top and bottom should also be included if A (or ϕ) are coupled to quarks. Therefore, the two-loop contribution is

$$(\Delta a_\ell^{\phi A})_{2\text{loop}} = -\frac{\alpha^2}{8\pi^2 \sin^2 \theta_W} \frac{m_\ell^2}{M_W^2} m_\tau^2 \left(\text{Re} \left(C_\phi^\ell C_\phi^{\tau*} \right) \frac{L_\phi^\tau}{M_\phi^2} - \text{Re} \left(C_A^\ell C_A^{\tau*} \right) \frac{L_A^\tau}{M_A^2} \right), \quad (5.5)$$

where the loop functions are

$$L_\phi^\tau = \int_0^1 dz \frac{1 - 2z(1-z)}{z(1-z) - r_\phi^\tau} \ln \frac{z(1-z)}{r_\phi^\tau}, \quad L_A^\tau = \int_0^1 dz \frac{1}{z(1-z) - r_A^\tau} \ln \frac{z(1-z)}{r_A^\tau}, \quad (5.6)$$

with asymptotic limits

$$L_\phi^\tau = \begin{cases} \frac{6 \ln r + 13}{9r} & r \gg 1 \\ \ln^2 r + 2 \ln r + 4 + \frac{\pi^3}{3} & r \ll 1 \end{cases}, \quad L_A^\tau = \begin{cases} \frac{\ln r + 2}{r} & r \gg 1 \\ \ln^2 r + \frac{\pi^3}{3} & r \ll 1. \end{cases} \quad (5.7)$$

As shown by eq. (5.5), two loop effects for Δa_ℓ exhibit NS and can be positive or negative depending on the sign of $\text{Re}(C^\ell C^{\tau*})$. Moreover, the enhancement factor $m_\tau^2/m_{e,\mu}^2$ of two loop effects relative to one-loop effects, which is particularly important for the case of the electron $g-2$, can easily compensate the additional loop suppression, as we will see later. On the other hand, in the case of the τ , one-loop effects are typically dominant compared to two-loop effects.

Hereafter, we will focus on the case of pseudoscalar particles, which is especially interesting. Specializing to the mass regime $m_\ell \ll M_A$ where the Δa_μ anomaly can find an explanation, we have the following situation: 1) Δa_e is always dominated by two-loop effects, 2) Δa_μ receives comparable one- and two-loop contributions, and 3) Δa_τ is always dominated by one-loop effects. As a result, we expect significant NS violations that we are going now to study numerically.

In the left plot of figure 6, we show the anatomy of the contributions to Δa_μ setting $C_A = 50$: the red line corresponds to the magnitude of the negative (“−”) one-loop effects, the green line refers to the positive (“+”) two-loop effects and the black line stands for the magnitude of the total contribution. The most prominent feature emerging from this plot is the different decoupling properties of the one- and two-loop effects as one can check

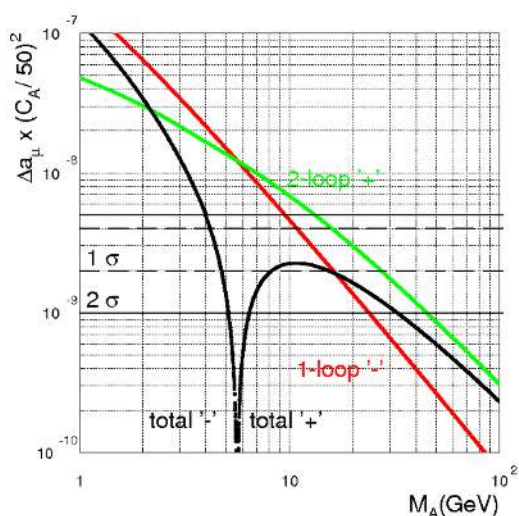


Figure 6. The different contributions to Δa_μ induced by a pseudoscalar particle (with mass M_A) as a function of M_A . The red line corresponds to the negative (“-”) one-loop contribution, the green line to the positive (“+”) two-loop contribution and the black line to the total effect.

directly from eq. (5.7). In particular, two-loop effects have a much milder decoupling with M_A compared to one loop-effects. This implies, in turn, the existence of a value for M_A where the two effects have comparable (and opposite) size. The exact value of M_A where this happens depends on the masses and couplings of the particles circulating in the second loop of the Barr-Zee diagram. In our case, an almost exact cancellation occurs for $M_A \approx 6$ GeV and therefore the total contribution to Δa_μ is positive for $M_A \gtrsim 6$ GeV and negative for $M_A \lesssim 6$ GeV.

In figure 7 we show the values attained by Δa_ℓ induced by pseudoscalar effects monitoring, in particular, whether NS is at work or not.

In the left plot of figure 7, we show Δa_μ vs. Δa_e for different pseudoscalar masses M_A and varying C_A . As we can see, NS (black line) is systematically violated by a large amount and, in particular, Δa_e always lies above its naive expectation. The actual amount of NS violations depends on the degree of cancellation between one- and two-loop effects entering Δa_μ . Overall, in the regions where the Δa_μ anomaly is accommodated, Δa_e typically exceeds the 10^{-13} level, thereby providing a splendid opportunity to test the $g-2$ anomaly via the electron one.

In figure 7, on the right, we show Δa_μ vs. Δa_τ for different pseudoscalar masses M_A and varying C_A . Similarly to the case of the electron $g-2$, NS (black line) is largely violated and Δa_τ can reach values up to the level of 10^{-3} , while explaining the Δa_μ anomaly. Such values should be well within the experimental resolutions expected at a SuperB factory.

Let us discuss now the predictions for the leptonic EDMs induced by light pseudoscalars. At one-loop level, the effective Lagrangian of eq. (5.1) leads to a real dipole amplitude and therefore the EDMs are vanishing at this order. Two loop effects are generally complex and provide very important contributions, as already discussed for the case of the leptonic $g-2$.

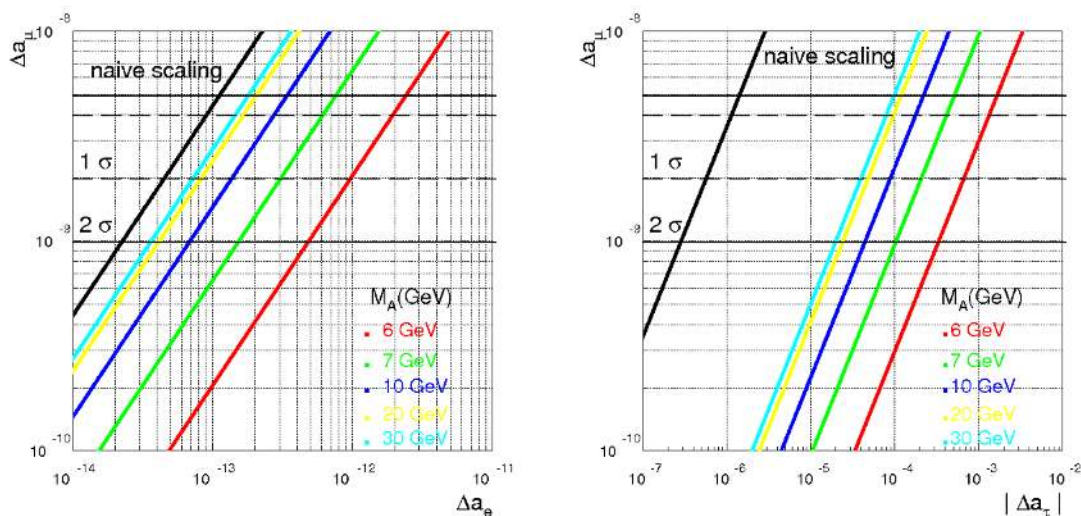


Figure 7. Left: Δa_μ vs. Δa_e for different values of M_A varying C_A . Right: Δa_μ vs. Δa_τ for different values of M_A varying C_A . The naive scaling predictions are given by black lines.

Since two-loop effects follow NS, it is expected that the electron EDM is the most sensitive probe of this scenario among the leptonic EDMs. In particular, from the *model-independent* expectations of eq. (3.12), we deduce that, in order to accommodate the $(g - 2)_\mu$ anomaly while satisfying the electron EDM bounds, we need the condition $\text{Im}(C^\ell C^{f*}) \lesssim 10^{-3}$, where f stands here for the heavy fermion running in the second loop. This condition could be naturally satisfied either if $\text{Im}(C^\ell) = \text{Im}(C^f)$ or if a dynamical mechanism suppresses both $\text{Im}(C^\ell)$ and $\text{Im}(C^f)$, for instance by a loop factor.

6 Vector-like fermions and a_e

In the following, we will consider the impact of heavy vector-like fermions on the leptonic $(g - 2)$ (see also [119]). The introduction of heavy vector-like fermions, mixing with the SM fermions, can be motivated by the explanation of flavor hierarchies in the SM, as we will discuss shortly.

Hereafter, we will focus on the leptonic sector only and therefore we introduce SU(2) vector-like doublets $(L_L \oplus L_R)$ and singlets $(E_L \oplus E_R)$ governed by the Lagrangian

$$\begin{aligned}
 -\mathcal{L} = & M_E \bar{E}_L E_R + M_L \bar{L}_R L_L + m_E \bar{E}_L e_R + m_L \bar{L}_R \ell_L \\
 & + \lambda_{LE} \bar{L}_L E_R H + \bar{\lambda}_{LE} \bar{L}_R E_L H^\dagger + \text{h.c.} .
 \end{aligned}
 \tag{6.1}$$

The fields L_L (L_R) and E_R (E_L) have the same (opposite) quantum numbers as the SM fields ℓ_L and e_R , respectively. Note that the SM Yukawas are assumed to be vanishing and they will be generated dynamically after electroweak symmetry breaking through the mixing between light and heavy fermions, once heavy fermions are integrated out.

The above Lagrangian is reminiscent of the fermionic sector of composite Higgs models which are dual of warped 5d models. In such a scheme, the chiral fermions correspond

to weakly-coupled elementary fields while the vector-like fermions are composite fields belonging to a strongly interacting sector. The Higgs boson also belongs to the strong sector and does not couple to elementary fields.

The mass eigenstates, before electroweak symmetry breaking, are obtained diagonalizing the mass mixing in \mathcal{L} through the following 2×2 unitary matrices

$$\begin{pmatrix} \ell_L \\ L_L \end{pmatrix} \rightarrow \begin{pmatrix} \cos \theta_L & \sin \theta_L \\ -\sin \theta_L & \cos \theta_L \end{pmatrix} \begin{pmatrix} \ell_L \\ L_L \end{pmatrix}, \quad \begin{pmatrix} e_R \\ E_R \end{pmatrix} \rightarrow \begin{pmatrix} \cos \theta_R & \sin \theta_R \\ -\sin \theta_R & \cos \theta_R \end{pmatrix} \begin{pmatrix} e_R \\ E_R \end{pmatrix}, \quad (6.2)$$

where

$$\tan \theta_L = \frac{m_L}{M_L}, \quad \tan \theta_R = \frac{m_E}{M_E}. \quad (6.3)$$

Hereafter we use the notation $s_{L(R)} = \sin \theta_{L(R)}$ and $c_{L(R)} = \cos \theta_{L(R)}$. After performing the rotations of eq. (6.2), the Lagrangian of eq. (6.1) becomes

$$-\mathcal{L} = M'_E \bar{E}_L E_R + M'_L \bar{L}_R L_L + \bar{\lambda}_{LE} \bar{L}_R E_L H^\dagger + \lambda_{LE} (s_{LSR} \bar{\ell}_L e_R + c_{LSR} \bar{L}_L e_R + s_{LCR} \bar{\ell}_L E_R + c_{LCR} \bar{L}_L E_R) H + \text{h.c.}, \quad (6.4)$$

where

$$M'_L = \sqrt{M_L^2 + m_L^2}, \quad M'_E = \sqrt{M_E^2 + m_E^2}, \quad (6.5)$$

and therefore we can define the following mass mixing matrix

$$M_\pm = \begin{matrix} & e_R & L_R & E_R \\ \ell_L & \lambda_{LESLSR} v & 0 & \lambda_{LESLCR} v \\ L_L & \lambda_{LECLSR} v & M'_L & \lambda_{LECRCR} v \\ E_L & 0 & \bar{\lambda}_{LE} v & M'_E \end{matrix}. \quad (6.6)$$

As a result, the fermionic spectrum consists of two heavy fermions with masses approximately given by M'_E and M'_L and light SM fermions with masses given by

$$m_{\ell_i} \simeq \lambda_{LE} s_L^i s_R^i v + \mathcal{O}\left(\frac{v^2}{M_{L,E}^2}\right), \quad (6.7)$$

where $i = 1, 2, 3$ is a lepton flavor index. The leptonic $g-2$ are generated at the loop-level by the exchange of the Higgs, W , Z bosons and heavy fermions. The dominant contribution arises from the diagram with an underlying mixing of $SU(2)$ doublets and singlets (since it is chirally enhanced by a factor of v/m_ℓ).

Using the mass relation of eq. (6.7), neglecting terms of order $\mathcal{O}(v^4/M_{L,E}^4)$ and performing an explicit loop calculation one can find that the dominant contribution is given by [119]

$$\Delta a_\ell \simeq \frac{c}{16\pi^2} \frac{m_\ell^2}{M_L M_E} \text{Re}(\lambda_{LE} \bar{\lambda}_{LE} c_{LCR}) \approx c \times 10^{-9} \text{Re}(\lambda_{LE} \bar{\lambda}_{LE}) \left(\frac{300 \text{ GeV}}{\sqrt{M_L M_E}}\right)^2 \frac{m_\ell^2}{m_\mu^2}. \quad (6.8)$$

where $c \sim \mathcal{O}(1)$. From eq. (6.8) we learn that if the heavy leptons have masses around the EW scale $M_L, M_E \sim v$ and if $\text{Re}(\lambda_{LE} \bar{\lambda}_{LE}) \sim 1$ then the muon $g-2$ anomaly can be

solved. We stress that, in general, the parameters λ_{LE} , $\bar{\lambda}_{LE}$, $M_{L,E}$, and $c_{L,R}$ are not flavor universal and therefore naive scaling might be violated.

The Yukawa couplings λ_{LE} and $\bar{\lambda}_{LE}$ could also violate lepton flavor and CP. As a reference framework, we consider the so-called anarchic scenario, where all the entries in λ_{LE} and $\bar{\lambda}_{LE}$ are assumed to be of order one. For the branching ratio of $\mu \rightarrow e\gamma$ we obtain

$$\text{BR}(\mu \rightarrow e\gamma) \approx c^2 \times 10^{-6} |\lambda_{LE} \bar{\lambda}_{LE}|^2 \left(\frac{300 \text{ GeV}}{\sqrt{M_L M_E}} \right)^4 \left(\frac{|s_L^e/s_L^\mu|^2 + |s_R^e/s_R^\mu|^2}{m_e/m_\mu} \right), \quad (6.9)$$

and therefore, in order to satisfy the experimental constraint $\text{BR}(\mu \rightarrow e\gamma) \lesssim 2 \times 10^{-12}$, we need $|s_{L(R)}^e/s_{L(R)}^\mu|^2 \lesssim 2 \times 10^{-6} \frac{m_e}{m_\mu}$ for $c \sim 1$. Such a suppression for the flavor mixing angles could be achieved by introducing a flavor symmetry determining the structures of λ_{LE} and $\bar{\lambda}_{LE}$.

For the electron EDM we find

$$\frac{d_e}{e} \approx 5c \times 10^{-25} \text{Im}(\lambda_{LE} \bar{\lambda}_{LE}) \left(\frac{300 \text{ GeV}}{\sqrt{M_L M_E}} \right)^2 e \text{ cm}, \quad (6.10)$$

and the experimental bound is satisfied for $|\text{Im}(\lambda_{LE} \bar{\lambda}_{LE})| \lesssim 2 \times 10^{-3}$ for $c \sim 1$. Thus, we conclude that both the flavor and CP structures of λ_{LE} and $\bar{\lambda}_{LE}$ have to be highly non-generic to satisfy the constraints from $\ell_i \rightarrow \ell_i \gamma$ and the electron EDM.

Finally, we mention that interactions with heavy leptons generate also corrections to the fermion couplings of the Z and Higgs bosons. Indeed, after integrating out the heavy states using their equations of motion we obtain dimension-six operators leading to corrections of the fermion couplings of the form $v^2/M_{L,E}^2$.

7 Conclusions

The aim of this paper was to show that the anomalous magnetic moment of the electron a_e can be viewed today as a new player among the low-energy processes that are able to probe new-physics effects. This novel status of a_e stems from recent improvements on both the experimental and theoretical fronts. One important ingredient is the measurement of α from atomic-physics experiments, which are becoming competitive with a_e in the determination of the fine-structure constant. The second ingredient is the ongoing effort to measure a_e with better experimental accuracy. The third element is a more precise theoretical determination of a_e in the SM. At present, the experimental measurement of a_e is in good agreement with the SM and the uncertainty in the quantity $\Delta a_e = a_e^{\text{EXP}} - a_e^{\text{SM}}$ is about 8×10^{-13} . As discussed in this paper, future progress can reduce this error by about one order of magnitude.

From the theoretical point of view, the great interest in testing new-physics effects in a_e comes from the well-known discrepancy between the experimental measurement and the SM prediction of a_μ . Observing or excluding an anomaly in a_e could become the most convincing way to establish the origin of the a_μ discrepancy. In a large class of models, new-physics contributions to a_ℓ (for $\ell = e, \mu, \tau$) are proportional to m_ℓ^2 , a situation that we call “naive scaling”. In the case of naive scaling, the present value of the $(g-2)_\mu$ anomaly,

see eq. (1.1), corresponds to $\Delta a_e = (0.7 \pm 0.2) \times 10^{-13}$. While theoretical predictions have recently achieved an impressive precision $\mathcal{O}(10^{-13})$ via formidable calculations, confirmation of the a_μ discrepancy through a_e still requires experimental improvements at the utmost level.

In many well-motivated cases, new physics effects do not respect naive scaling, as we have shown with several examples of such theories. In the context of supersymmetry, this can happen with lepton flavor conservation (for non-degenerate but aligned sleptons) or with lepton flavor violation (with relative misalignment between lepton and sleptons). In the first case, once we normalize Δa_e in such a way to reproduce $\Delta a_\mu \approx 3 \times 10^{-9}$, we obtain specific predictions on violation of lepton universality in $P \rightarrow \mu\nu/P \rightarrow e\nu$ and $P \rightarrow \mu\nu/\tau \rightarrow P\nu$, for $P = \pi, K$. The case of lepton flavor violation cannot explain the anomaly in a_μ , but can lead to new effects in a_e that are correlated with the prediction of $\tau \rightarrow e\gamma$ and violation of e/μ lepton universality. In a fairly model-independent way, it is also possible to correlate new effects in Δa_e with the corresponding electric dipole moment.

We have also considered a class of theories with a light (pseudo)scalar interacting with matter proportionally to ordinary Yukawa couplings. In this case we have found an interesting pattern of violations of naive scaling coming from the interplay between one-loop contributions with $\Delta a_\ell \propto m_\ell^4$ and two-loop contributions with $\Delta a_\ell \propto m_\ell^2$. For the parameters capable of explaining the $(g-2)_\mu$ anomaly, we found that Δa_e is larger than its naive-scaling value and can be close to its present experimental bound.

We believe that a_e offers a special opportunity to test new-physics effects and to shed new light on the current discrepancy in the muon anomalous magnetic moment. A robust and ambitious experimental program is necessary to exploit its full potential.

Acknowledgments

We would like to thank L. Mercolli for participating in the early stages of this work. We are also grateful to G. Gabrielse, T. Kinoshita, W. J. Marciano, F. Nez, D. Straub, A. Strumia, and S. K. Vempati for fruitful discussions and correspondence. M.P. also thanks the Department of Physics of the University of Padova for its support. His work was supported in part by the Italian Ministero dell'Università e della Ricerca Scientifica under the COFIN program PRIN 2008, and by the European Programmes UNILHC (contract PITN-GA-2009-237920) and INVISIBLES (contract PITN-GA-2011-289442).

A Loop functions

The loop functions entering the supersymmetric contributions $\Delta a_\ell^{\text{LFC}}$, $\Delta a_\ell^{\text{LFV}}$, and $\text{BR}(\ell_i \rightarrow \ell_j \gamma)$ are given by

$$f_n(x) = \frac{1 - x^2 + 2x \log x}{(1 - x)^3}, \tag{A.1}$$

$$f_c(x) = \frac{3 - 4x + x^2 + 2 \log x}{(x - 1)^3}, \tag{A.2}$$

$$g_n(x) = \frac{1 + 4x - 5x^2 + 2x(x + 2) \log x}{4(1 - x)^4}, \quad (\text{A.3})$$

$$g_c(x) = \frac{5 - 4x - x^2 + 2(2x + 1) \log x}{2(1 - x)^4}, \quad (\text{A.4})$$

$$h_n(x) = \frac{1 + 9x - 9x^2 - x^3 + 6x(x + 1) \log x}{3(1 - x)^5}, \quad (\text{A.5})$$

$$l_n(x) = \frac{3 + 44x - 36x^2 - 12x^3 + x^4 + 12x(3x + 2) \log x}{6(1 - x)^6}, \quad (\text{A.6})$$

We have also defined $f_{(c,n)}(x, y) = f_{(c,n)}(x) - f_{(c,n)}(y)$.

Open Access. This article is distributed under the terms of the Creative Commons Attribution License which permits any use, distribution and reproduction in any medium, provided the original author(s) and source are credited.

References

- [1] MUON G-2 collaboration, G. Bennett et al., *Final Report of the Muon E821 Anomalous Magnetic Moment Measurement at BNL*, *Phys. Rev. D* **73** (2006) 072003 [[hep-ex/0602035](#)] [[INSPIRE](#)].
- [2] MUON G-2 collaboration, G. Bennett et al., *Measurement of the negative muon anomalous magnetic moment to 0.7 ppm*, *Phys. Rev. Lett.* **92** (2004) 161802 [[hep-ex/0401008](#)] [[INSPIRE](#)].
- [3] MUON G-2 collaboration, G. Bennett et al., *Measurement of the positive muon anomalous magnetic moment to 0.7 ppm*, *Phys. Rev. Lett.* **89** (2002) 101804 [Erratum *ibid.* **89** (2002) 129903] [[hep-ex/0208001](#)] [[INSPIRE](#)].
- [4] MUON G-2 collaboration, H. Brown et al., *Precise measurement of the positive muon anomalous magnetic moment*, *Phys. Rev. Lett.* **86** (2001) 2227 [[hep-ex/0102017](#)] [[INSPIRE](#)].
- [5] F. Jegerlehner and A. Nyffeler, *The Muon g-2*, *Phys. Rept.* **477** (2009) 1 [[arXiv:0902.3360](#)] [[INSPIRE](#)].
- [6] K. Hagiwara, R. Liao, A.D. Martin, D. Nomura and T. Teubner, *$(g - 2)_\mu$ and $\alpha(M_Z^2)$ re-evaluated using new precise data*, *J. Phys. G* **38** (2011) 085003 [[arXiv:1105.3149](#)] [[INSPIRE](#)].
- [7] M. Davier, A. Hoecker, B. Malaescu and Z. Zhang, *Reevaluation of the Hadronic Contributions to the Muon g-2 and to α_{MZ}* , *Eur. Phys. J. C* **71** (2011) 1515 [Erratum *ibid.* **C 72** (2012) 1874] [[arXiv:1010.4180](#)] [[INSPIRE](#)].
- [8] R. Van Dyck, P. Schwinberg and H. Dehmelt, *New High Precision Comparison of electron and Positron G Factors*, *Phys. Rev. Lett.* **59** (1987) 26 [[INSPIRE](#)].
- [9] P. Mohr and B. Taylor, *CODATA recommended values of the fundamental physical constants: 1998*, *Rev. Mod. Phys.* **72** (2000) 351 [[INSPIRE](#)].
- [10] D. Hanneke, S. Fogwell and G. Gabrielse, *New Measurement of the Electron Magnetic Moment and the Fine Structure Constant*, *Phys. Rev. Lett.* **100** (2008) 120801 [[arXiv:0801.1134](#)] [[INSPIRE](#)].

- [11] B.C. Odom, D. Hanneke, B. D’Urso and G. Gabrielse, *New Measurement of the Electron Magnetic Moment Using a One-Electron Quantum Cyclotron*, *Phys. Rev. Lett.* **97** (2006) 030801 [Erratum *ibid.* **99** (2007) 039902] [INSPIRE].
- [12] D. Hanneke, S.F. Hoogerheide and G. Gabrielse, *Cavity Control of a Single-Electron Quantum Cyclotron: Measuring the Electron Magnetic Moment*, *Phys. Rev.* **A 83** (2011) 052122.
- [13] T. Kinoshita and W.J. Marciano, *Theory of the anomalous magnetic moment of the muon*, in *Quantum Electrodynamics*, edited by T. Kinoshita, World Scientific (1990), pp. 419–478.
- [14] J.S. Schwinger, *On Quantum electrodynamics and the magnetic moment of the electron*, *Phys. Rev.* **73** (1948) 416 [INSPIRE].
- [15] C.M. Sommerfield, *Magnetic Dipole Moment of the Electron*, *Phys. Rev.* **107** (1957) 328 [INSPIRE].
- [16] C.M. Sommerfield, *The magnetic moment of the electron*, *Ann. Phys.* **5** (1958) 26.
- [17] A. Petermann, *Fourth order magnetic moment of the electron*, *Helv. Phys. Acta* **30** (1957) 407 [INSPIRE].
- [18] A. Petermann, *Fourth order magnetic moment of the electron*, *Nucl. Phys.* **5** (1958) 677.
- [19] H.H. Elend, *On the anomalous magnetic moment of the muon*, *Phys. Lett.* **20** (1966) 682 [Erratum *ibid.* **21** (1966) 720].
- [20] M. Passera, *The Standard model prediction of the muon anomalous magnetic moment*, *J. Phys.* **G 31** (2005) R75 [hep-ph/0411168] [INSPIRE].
- [21] P.J. Mohr, B.N. Taylor and D.B. Newell, *CODATA Recommended Values of the Fundamental Physical Constants: 2010*, arXiv:1203.5425 [INSPIRE].
- [22] S. Laporta and E. Remiddi, *The Analytical value of the electron ($g-2$) at order α^3 in QED*, *Phys. Lett.* **B 379** (1996) 283 [hep-ph/9602417] [INSPIRE].
- [23] S. Laporta, *The Analytical contribution of the sixth order graphs with vacuum polarization insertions to the muon ($g-2$) in QED*, *Nuovo Cim.* **A 106** (1993) 675 [INSPIRE].
- [24] S. Laporta and E. Remiddi, *The Analytical value of the electron light-light graphs contribution to the muon ($g-2$) in QED*, *Phys. Lett.* **B 301** (1993) 440 [INSPIRE].
- [25] E. Remiddi and J. Vermaseren, *Harmonic polylogarithms*, *Int. J. Mod. Phys.* **A 15** (2000) 725 [hep-ph/9905237] [INSPIRE].
- [26] T. Gehrmann and E. Remiddi, *Numerical evaluation of harmonic polylogarithms*, *Comput. Phys. Commun.* **141** (2001) 296 [hep-ph/0107173] [INSPIRE].
- [27] T. Gehrmann and E. Remiddi, *Numerical evaluation of two-dimensional harmonic polylogarithms*, *Comput. Phys. Commun.* **144** (2002) 200 [hep-ph/0111255] [INSPIRE].
- [28] D. Maître, *HPL, a mathematica implementation of the harmonic polylogarithms*, *Comput. Phys. Commun.* **174** (2006) 222 [hep-ph/0507152] [INSPIRE].
- [29] M. Passera, *Precise mass-dependent QED contributions to leptonic $g-2$ at order α^2 and α^3* , *Phys. Rev.* **D 75** (2007) 013002 [hep-ph/0606174] [INSPIRE].
- [30] M.A. Samuel and G. Li, *Improved analytic theory of the muon anomalous magnetic moment*, *Phys. Rev.* **D 44** (1991) 3935 [Erratum *ibid.* **D 46** (1992) 4782] [Erratum *ibid.* **D 48** (1993) 1879] [INSPIRE].

- [31] T. Aoyama, M. Hayakawa, T. Kinoshita and M. Nio, *Revised value of the eighth-order electron $g-2$* , *Phys. Rev. Lett.* **99** (2007) 110406 [[arXiv:0706.3496](#)] [[INSPIRE](#)].
- [32] T. Aoyama, M. Hayakawa, T. Kinoshita and M. Nio, *Revised value of the eighth-order QED contribution to the anomalous magnetic moment of the electron*, *Phys. Rev.* **D 77** (2008) 053012 [[arXiv:0712.2607](#)] [[INSPIRE](#)].
- [33] T. Aoyama, M. Hayakawa, T. Kinoshita and M. Nio, *Tenth-Order QED Contribution to the Electron $g-2$ and an Improved Value of the Fine Structure Constant*, *Phys. Rev. Lett.* **109** (2012) 111807 [[arXiv:1205.5368](#)] [[INSPIRE](#)].
- [34] S. Laporta and E. Remiddi, *Status of the QED prediction of the electron ($g - 2$)*, *Nucl. Phys. Proc. Suppl.* **181-182** (2008) 10 [[INSPIRE](#)].
- [35] T. Kinoshita and M. Nio, *The Tenth-order QED contribution to the lepton $g-2$: Evaluation of dominant α^5 terms of muon $g-2$* , *Phys. Rev.* **D 73** (2006) 053007 [[hep-ph/0512330](#)] [[INSPIRE](#)].
- [36] T. Aoyama, M. Hayakawa, T. Kinoshita and M. Nio, *Automated calculation scheme for α^n contributions of QED to lepton $g-2$: Generating renormalized amplitudes for diagrams without lepton loops*, *Nucl. Phys.* **B 740** (2006) 138 [[hep-ph/0512288](#)] [[INSPIRE](#)].
- [37] T. Aoyama, M. Hayakawa, T. Kinoshita and M. Nio, *Automated calculation scheme for α^n contributions of QED to lepton $g-2$: New treatment of infrared divergence for diagrams without lepton loops*, *Nucl. Phys.* **B 796** (2008) 184 [[arXiv:0709.1568](#)] [[INSPIRE](#)].
- [38] T. Aoyama, M. Hayakawa, T. Kinoshita and M. Nio, *Tenth-Order Lepton Anomalous Magnetic Moment: Second-Order Vertex Containing Two Vacuum Polarization Subdiagrams, One Within the Other*, *Phys. Rev.* **D 78** (2008) 113006 [[arXiv:0810.5208](#)] [[INSPIRE](#)].
- [39] T. Aoyama, M. Hayakawa, T. Kinoshita and M. Nio, *Tenth-order lepton $g-2$: Contribution of some fourth-order radiative corrections to the sixth-order $g-2$ containing light-by-light-scattering subdiagrams*, *Phys. Rev.* **D 82** (2010) 113004 [[arXiv:1009.3077](#)] [[INSPIRE](#)].
- [40] T. Aoyama, M. Hayakawa, T. Kinoshita and M. Nio, *Proper Eighth-Order Vacuum-Polarization Function and its Contribution to the Tenth-Order Lepton $g-2$* , *Phys. Rev.* **D 83** (2011) 053003 [[arXiv:1012.5569](#)] [[INSPIRE](#)].
- [41] T. Aoyama, M. Hayakawa, T. Kinoshita and M. Nio, *Tenth-Order QED contribution to Lepton Anomalous Magnetic Moment - Fourth-Order Vertices Containing Sixth-Order Vacuum-Polarization Subdiagrams*, *Phys. Rev.* **D 83** (2011) 053002 [[arXiv:1101.0459](#)] [[INSPIRE](#)].
- [42] T. Aoyama, M. Hayakawa, T. Kinoshita and M. Nio, *Tenth-Order Lepton Anomalous Magnetic Moment — Sixth-Order Vertices Containing Vacuum-Polarization Subdiagrams*, *Phys. Rev.* **D 84** (2011) 053003 [[arXiv:1105.5200](#)] [[INSPIRE](#)].
- [43] T. Aoyama, M. Hayakawa, T. Kinoshita and M. Nio, *Tenth-Order QED Lepton Anomalous Magnetic Moment — Eighth-Order Vertices Containing a Second-Order Vacuum Polarization*, *Phys. Rev.* **D 85** (2012) 033007 [[arXiv:1110.2826](#)] [[INSPIRE](#)].
- [44] T. Aoyama, M. Hayakawa, T. Kinoshita and M. Nio, *Tenth-Order QED Contribution to the Lepton Anomalous Magnetic Moment — Sixth-Order Vertices Containing an Internal*

- Light-by-Light-Scattering Subdiagram*, *Phys. Rev. D* **85** (2012) 093013 [[arXiv:1201.2461](#)] [[INSPIRE](#)].
- [45] T. Aoyama, M. Hayakawa, T. Kinoshita, M. Nio and N. Watanabe, *Eighth-Order Vacuum-Polarization Function Formed by Two Light-by-Light-Scattering Diagrams and its Contribution to the Tenth-Order Electron $g-2$* , *Phys. Rev. D* **78** (2008) 053005 [[arXiv:0806.3390](#)] [[INSPIRE](#)].
- [46] T. Aoyama et al., *Tenth-order lepton $g-2$: Contribution from diagrams containing sixth-order light-by-light-scattering subdiagram internally*, *Phys. Rev. D* **81** (2010) 053009 [[arXiv:1001.3704](#)] [[INSPIRE](#)].
- [47] A. Czarnecki, B. Krause and W.J. Marciano, *Electroweak corrections to the muon anomalous magnetic moment*, *Phys. Rev. Lett.* **76** (1996) 3267 [[hep-ph/9512369](#)] [[INSPIRE](#)].
- [48] A. Czarnecki, B. Krause and W.J. Marciano, *Electroweak Fermion loop contributions to the muon anomalous magnetic moment*, *Phys. Rev. D* **52** (1995) 2619 [[hep-ph/9506256](#)] [[INSPIRE](#)].
- [49] D. Nomura and T. Teubner, *Hadronic contributions to the anomalous magnetic moment of the electron and the hyperfine splitting of muonium*, [arXiv:1208.4194](#) [[INSPIRE](#)].
- [50] B. Krause, *Higher order hadronic contributions to the anomalous magnetic moment of leptons*, *Phys. Lett. B* **390** (1997) 392 [[hep-ph/9607259](#)] [[INSPIRE](#)].
- [51] J. Prades, E. de Rafael and A. Vainshtein, *Hadronic Light-by-Light Scattering Contribution to the Muon Anomalous Magnetic Moment*, in B.L. Roberts and W.J. Marciano (eds.), *Lepton dipole moments*, Advanced series on directions in high energy physics, Vol. 20, World Scientific (2010), pp. 303–317.
- [52] PARTICLE DATA GROUP collaboration, J. Beringer et al., *Review of Particle Physics (RPP)*, *Phys. Rev. D* **86** (2012) 010001 [[INSPIRE](#)].
- [53] V. Gerginov et al., *Optical frequency measurements of $6s^2S_{1/2} - 6p^2P_{1/2}(D_1)$ transitions in Cs-133 and their impact on the fine-structure constant*, *Phys. Rev. A* **73** (2006) 032504 [[INSPIRE](#)].
- [54] P. Clade et al., *Determination of the Fine Structure Constant Based on Bloch Oscillations of Ultracold Atoms in a Vertical Optical Lattice*, *Phys. Rev. Lett.* **96** (2006) 033001 [[INSPIRE](#)].
- [55] M. Cadoret et al., *Combination of Bloch oscillations with a Ramsey-Borde interferometer: New determination of the fine structure constant*, *Phys. Rev. Lett.* **101** (2008) 230801 [[arXiv:0810.3152](#)] [[INSPIRE](#)].
- [56] R. Bouchendira, P. Clade, S. Guellati-Khelifa, F. Nez and F. Biraben, *New determination of the fine structure constant and test of the quantum electrodynamics*, *Phys. Rev. Lett.* **106** (2011) 080801 [[arXiv:1012.3627](#)] [[INSPIRE](#)].
- [57] T. Kinoshita, *In search of the breakdown of QED: Study of lepton $g-2$ from 1947 to present*, in B.L. Roberts and W.J. Marciano (eds.), *Lepton dipole moments*, Advanced series on directions in high energy physics, Vol. 20, World Scientific (2010), pp. 69–117.
- [58] G. Gabrielse, *In search of the breakdown of QED: Study of lepton $g-2$ from 1947 to present*, in B.L. Roberts and W.J. Marciano (eds.), *Lepton dipole moments*, Advanced series on directions in high energy physics, Vol. 20, World Scientific (2010), pp. 157–218.
- [59] G. Gabrielse, private communication.

- [60] F. Nez, private communication.
- [61] Y.K. Semertzidis, *Review of EDM experiments*, *J. Phys. Conf. Ser.* **335** (2011) 012012 [[INSPIRE](#)].
- [62] M. Raidal et al., *Flavour physics of leptons and dipole moments*, *Eur. Phys. J. C* **57** (2008) 13 [[arXiv:0801.1826](#)] [[INSPIRE](#)].
- [63] S. Eidelman and M. Passera, *Theory of the tau lepton anomalous magnetic moment*, *Mod. Phys. Lett. A* **22** (2007) 159 [[hep-ph/0701260](#)] [[INSPIRE](#)].
- [64] DELPHI collaboration, J. Abdallah et al., *Study of tau-pair production in photon-photon collisions at LEP and limits on the anomalous electromagnetic moments of the tau lepton*, *Eur. Phys. J. C* **35** (2004) 159 [[hep-ex/0406010](#)] [[INSPIRE](#)].
- [65] G.A. Gonzalez-Sprinberg, A. Santamaria and J. Vidal, *Model independent bounds on the tau lepton electromagnetic and weak magnetic moments*, *Nucl. Phys. B* **582** (2000) 3 [[hep-ph/0002203](#)] [[INSPIRE](#)].
- [66] T. Aushev et al., *Physics at Super B Factory*, [arXiv:1002.5012](#) [[INSPIRE](#)].
- [67] A. Lusiani, *Tau physics at SuperB*, *Nucl. Phys. Proc. Suppl.* **218** (2011) 335 [[INSPIRE](#)].
- [68] J. Bernabeu, G. Gonzalez-Sprinberg, J. Papavassiliou and J. Vidal, *Tau anomalous magnetic moment form-factor at super B/ flavor factories*, *Nucl. Phys. B* **790** (2008) 160 [[arXiv:0707.2496](#)] [[INSPIRE](#)].
- [69] J. Bernabeu, G. Gonzalez-Sprinberg and J. Vidal, *Tau spin correlations and the anomalous magnetic moment*, *JHEP* **01** (2009) 062 [[arXiv:0807.2366](#)] [[INSPIRE](#)].
- [70] M. Fael, *Study of the anomalous magnetic moment of the τ lepton via its radiative leptonic decays*, M.Sc. Thesis (2010), University of Padua, Italy.
- [71] M. Laursen, M.A. Samuel and A. Sen, *Radiation zeros and a test for the g value of the tau lepton*, *Phys. Rev. D* **29** (1984) 2652 [*Erratum ibid.* **D 56** (1997) 3155] [[INSPIRE](#)].
- [72] S. Eidelman, D. Epifanov, M. Fael, L. Mercolli, C. Ng and M. Passera, in preparation.
- [73] Y. Nir and N. Seiberg, *Should squarks be degenerate?*, *Phys. Lett. B* **309** (1993) 337 [[hep-ph/9304307](#)] [[INSPIRE](#)].
- [74] M. Leurer, Y. Nir and N. Seiberg, *Mass matrix models: The Sequel*, *Nucl. Phys. B* **420** (1994) 468 [[hep-ph/9310320](#)] [[INSPIRE](#)].
- [75] T. Moroi, *The Muon anomalous magnetic dipole moment in the minimal supersymmetric standard model*, *Phys. Rev. D* **53** (1996) 6565 [*Erratum ibid.* **D 56** (1997) 4424] [[hep-ph/9512396](#)] [[INSPIRE](#)].
- [76] S. Dimopoulos and G. Giudice, *Naturalness constraints in supersymmetric theories with nonuniversal soft terms*, *Phys. Lett. B* **357** (1995) 573 [[hep-ph/9507282](#)] [[INSPIRE](#)].
- [77] A.G. Cohen, D. Kaplan and A. Nelson, *The More minimal supersymmetric standard model*, *Phys. Lett. B* **388** (1996) 588 [[hep-ph/9607394](#)] [[INSPIRE](#)].
- [78] P.H. Chankowski et al., *Delta R in the MSSM*, *Nucl. Phys. B* **417** (1994) 101 [[INSPIRE](#)].
- [79] P. Krawczyk and S. Pokorski, *Strongly Coupled Charged Scalar in B and t Decays*, *Phys. Rev. Lett.* **60** (1988) 182 [[INSPIRE](#)].

- [80] P.H. Chankowski, R. Hempfling and S. Pokorski, $\tau - \mu - e$ universality in tau decays and constraints on the slepton masses, *Phys. Lett. B* **333** (1994) 403 [[hep-ph/9405281](#)] [[INSPIRE](#)].
- [81] Y. Grossman, *Phenomenology of models with more than two Higgs doublets*, *Nucl. Phys. B* **426** (1994) 355 [[hep-ph/9401311](#)] [[INSPIRE](#)].
- [82] D. Britton et al., *Measurement of the $\pi^+ \rightarrow e^+$ neutrino branching ratio*, *Phys. Rev. Lett.* **68** (1992) 3000 [[INSPIRE](#)].
- [83] G. Czapke et al., *Branching ratio for the rare pion decay into positron and neutrino*, *Phys. Rev. Lett.* **70** (1993) 17 [[INSPIRE](#)].
- [84] NA62 collaboration, C. Lazzeroni et al., *Test of Lepton Flavour Universality in $K^+ \rightarrow l^+ \nu$ Decays*, *Phys. Lett. B* **698** (2011) 105 [[arXiv:1101.4805](#)] [[INSPIRE](#)].
- [85] M. Antonelli et al., *An Evaluation of $|V_{us}|$ and precise tests of the Standard Model from world data on leptonic and semileptonic kaon decays*, *Eur. Phys. J. C* **69** (2010) 399 [[arXiv:1005.2323](#)] [[INSPIRE](#)].
- [86] ALEPH, CDF, D0, DELPHI, L3, OPAL, SLD collaborations, LEP, Tevatron Electroweak Working Group, SLD Electroweak and Heavy Flavour Groups collaboration, *Precision Electroweak Measurements and Constraints on the Standard Model*, [arXiv:1012.2367](#) [[INSPIRE](#)].
- [87] <http://www.cern.ch/LEPEWWG/>.
- [88] ALEPH, DELPHI, L3, OPAL, SLD collaborations, LEP Electroweak Working Group, SLD Electroweak Group, SLD Heavy Flavour Group collaboration, S. Schael et al., *Precision electroweak measurements on the Z resonance*, *Phys. Rept.* **427** (2006) 257 [[hep-ex/0509008](#)] [[INSPIRE](#)].
- [89] ALEPH, DELPHI, L3, OPAL collaborations, LEP Electroweak Working Group, SLD Heavy Flavor and Electroweak Groups collaboration, D. Abbaneo et al., *A Combination of preliminary electroweak measurements and constraints on the standard model*, [hep-ex/0112021](#) [[INSPIRE](#)].
- [90] BABAR collaboration, B. Aubert et al., *Measurements of Charged Current Lepton Universality and $|V_{us}|$ using Tau Lepton Decays to $e^- \bar{\nu}_e n \nu_\tau$, $\mu^- \bar{n} \nu_\mu \nu_\tau$, $\pi^- \nu_\tau$ and $K^- \nu_\tau$* , *Phys. Rev. Lett.* **105** (2010) 051602 [[arXiv:0912.0242](#)] [[INSPIRE](#)].
- [91] SUPERB collaboration, M. Bona et al., *SuperB: A High-Luminosity Asymmetric e^+e^- Super Flavor Factory. Conceptual Design Report*, [arXiv:0709.0451](#) [[INSPIRE](#)].
- [92] MEG collaboration, J. Adam et al., *New limit on the lepton-flavour violating decay $\mu^+ \rightarrow e^+ \gamma$* , *Phys. Rev. Lett.* **107** (2011) 171801 [[arXiv:1107.5547](#)] [[INSPIRE](#)].
- [93] BABAR collaboration, B. Aubert et al., *Searches for Lepton Flavor Violation in the Decays $\tau^\pm \rightarrow e^\pm \gamma$ and $\tau^\pm \rightarrow \mu^\pm \gamma$* , *Phys. Rev. Lett.* **104** (2010) 021802 [[arXiv:0908.2381](#)] [[INSPIRE](#)].
- [94] BABAR collaboration, B. Aubert et al., *Improved limits on lepton flavor violating tau decays to $l\phi$, $l\rho$, lK^* and $l\bar{K}^*$* , *Phys. Rev. Lett.* **103** (2009) 021801 [[arXiv:0904.0339](#)] [[INSPIRE](#)].
- [95] BABAR collaboration, B. Aubert et al., *Search for lepton flavor violating decays $\tau^\pm \rightarrow l^\pm \omega$ ($l = e, \mu$)*, *Phys. Rev. Lett.* **100** (2008) 071802 [[arXiv:0711.0980](#)] [[INSPIRE](#)].

- [96] BABAR collaboration, B. Aubert et al., *Improved limits on the lepton-flavor violating decays $\tau^- \rightarrow \ell^- \ell^+ \ell^-$* , *Phys. Rev. Lett.* **99** (2007) 251803 [[arXiv:0708.3650](#)] [[INSPIRE](#)].
- [97] BABAR collaboration, B. Aubert et al., *Search for Lepton Flavor Violating Decays $\tau^\pm \rightarrow \ell^\pm \pi^0, \ell^\pm \eta, \ell^\pm \eta'$* , *Phys. Rev. Lett.* **98** (2007) 061803 [[hep-ex/0610067](#)] [[INSPIRE](#)].
- [98] BABAR collaboration, B. Aubert et al., *Search for lepton-flavor and lepton-number violation in the decay $\tau^- \rightarrow \ell^\mp h^\pm h'^-$* , *Phys. Rev. Lett.* **95** (2005) 191801 [[hep-ex/0506066](#)] [[INSPIRE](#)].
- [99] BABAR collaboration, J. Lees et al., *Limits on tau Lepton-Flavor Violating Decays in three charged leptons*, *Phys. Rev.* **D 81** (2010) 111101 [[arXiv:1002.4550](#)] [[INSPIRE](#)].
- [100] BABAR collaboration, B. Aubert et al., *Search for Lepton Flavor Violating Decays $\tau \rightarrow l^- K_s^0$ with the BABAR Experiment*, *Phys. Rev.* **D 79** (2009) 012004 [[arXiv:0812.3804](#)] [[INSPIRE](#)].
- [101] BELLE collaboration, Y. Miyazaki et al., *Search for Lepton Flavor Violating tau- Decays into $\ell - K^0 s$ and $\ell - K^0 s K^0 s$* , *Phys. Lett.* **B 692** (2010) 4 [[arXiv:1003.1183](#)] [[INSPIRE](#)].
- [102] K. Hayasaka et al., *Search for Lepton Flavor Violating Tau Decays into Three Leptons with 719 Million Produced Tau+Tau- Pairs*, *Phys. Lett.* **B 687** (2010) 139 [[arXiv:1001.3221](#)] [[INSPIRE](#)].
- [103] BELLE collaboration, Y. Miyazaki et al., *Search for Lepton Flavor and Lepton Number Violating tau Decays into a Lepton and Two Charged Mesons*, *Phys. Lett.* **B 682** (2010) 355 [[arXiv:0908.3156](#)] [[INSPIRE](#)].
- [104] BELLE collaboration, Y. Miyazaki et al., *Search for Lepton-Flavor-Violating tau Decays into Lepton and $f_0(980)$ Meson*, *Phys. Lett.* **B 672** (2009) 317 [[arXiv:0810.3519](#)] [[INSPIRE](#)].
- [105] BELLE collaboration, K. Hayasaka et al., *New search for $\tau \rightarrow \mu \gamma$ and $\tau \rightarrow e \gamma$ decays at Belle*, *Phys. Lett.* **B 666** (2008) 16 [[arXiv:0705.0650](#)] [[INSPIRE](#)].
- [106] BELLE collaboration, Y. Nishio et al., *Search for lepton-flavor-violating $\tau \rightarrow IV^0$ decays at Belle*, *Phys. Lett.* **B 664** (2008) 35 [[arXiv:0801.2475](#)] [[INSPIRE](#)].
- [107] BELLE collaboration, Y. Miyazaki et al., *Search for Lepton Flavor Violating tau Decays into Three Leptons*, *Phys. Lett.* **B 660** (2008) 154 [[arXiv:0711.2189](#)] [[INSPIRE](#)].
- [108] BELLE collaboration, Y. Miyazaki et al., *Search for lepton flavor violating τ^- decays into $l^- \eta, l^- \eta'$ and $l^- \pi^0$* , *Phys. Lett.* **B 648** (2007) 341 [[hep-ex/0703009](#)] [[INSPIRE](#)].
- [109] J. Hisano, T. Moroi, K. Tobe and M. Yamaguchi, *Lepton flavor violation via right-handed neutrino Yukawa couplings in supersymmetric standard model*, *Phys. Rev.* **D 53** (1996) 2442 [[hep-ph/9510309](#)] [[INSPIRE](#)].
- [110] P. Paradisi, *Constraints on SUSY lepton flavor violation by rare processes*, *JHEP* **10** (2005) 006 [[hep-ph/0505046](#)] [[INSPIRE](#)].
- [111] A. Masiero, P. Paradisi and R. Petronzio, *Probing new physics through $\mu - e$ universality in $K \rightarrow l \nu$* , *Phys. Rev.* **D 74** (2006) 011701 [[hep-ph/0511289](#)] [[INSPIRE](#)].
- [112] A. Masiero, P. Paradisi and R. Petronzio, *Anatomy and Phenomenology of the Lepton Flavor Universality in SUSY Theories*, *JHEP* **11** (2008) 042 [[arXiv:0807.4721](#)] [[INSPIRE](#)].
- [113] J. Hisano, M. Nagai and P. Paradisi, *Flavor effects on the electric dipole moments in supersymmetric theories: A beyond leading order analysis*, *Phys. Rev.* **D 80** (2009) 095014 [[arXiv:0812.4283](#)] [[INSPIRE](#)].

- [114] B. Bellazzini, Y. Grossman, I. Nachshon and P. Paradisi, *Non-Standard Neutrino Interactions at One Loop*, *JHEP* **06** (2011) 104 [[arXiv:1012.3759](#)] [[INSPIRE](#)].
- [115] G.F. Giudice, G. Isidori and P. Paradisi, *Direct CP-violation in charm and flavor mixing beyond the SM*, *JHEP* **04** (2012) 060 [[arXiv:1201.6204](#)] [[INSPIRE](#)].
- [116] B. Keren-Zur et al., *On Partial Compositeness and the CP asymmetry in charm decays*, *Nucl. Phys.* **B 867** (2013) 394 [[arXiv:1205.5803](#)] [[INSPIRE](#)].
- [117] U. Ellwanger, C. Hugonie and A.M. Teixeira, *The Next-to-Minimal Supersymmetric Standard Model*, *Phys. Rept.* **496** (2010) 1 [[arXiv:0910.1785](#)] [[INSPIRE](#)].
- [118] J.P. Leveille, *The Second Order Weak Correction to $(G-2)$ of the Muon in Arbitrary Gauge Models*, *Nucl. Phys.* **B 137** (1978) 63 [[INSPIRE](#)].
- [119] K. Kannike, M. Raidal, D.M. Straub and A. Strumia, *Anthropic solution to the magnetic muon anomaly: the charged see-saw*, *JHEP* **02** (2012) 106 [Erratum *ibid.* **1210** (2012) 136] [[arXiv:1111.2551](#)] [[INSPIRE](#)].
- [120] I. Masina and C.A. Savoy, *Sleptonarium: Constraints on the CP and flavor pattern of scalar lepton masses*, *Nucl. Phys.* **B 661** (2003) 365 [[hep-ph/0211283](#)] [[INSPIRE](#)].
- [121] J. Gierbach, S. Mertens, U. Nierste and S. Wiesenfeldt, *Lepton flavour violation in the MSSM*, *JHEP* **05** (2010) 026 [[arXiv:0910.2663](#)] [[INSPIRE](#)].
- [122] H. Davoudiasl, H.-S. Lee and W.J. Marciano, *Dark Side of Higgs Diphoton Decays and Muon $g-2$* , [arXiv:1208.2973](#) [[INSPIRE](#)].
- [123] M. Endo, K. Hamaguchi and G. Mishima, *Constraints on Hidden Photon Models from Electron $g-2$ and Hydrogen Spectroscopy*, [arXiv:1209.2558](#) [[INSPIRE](#)].